Available online at www.sciencedirect.com
SCIENCE DIRECT
Biochimica et Biophysica Acta 1716 (2005) 77 – 96
BIOCHIMICA ET BIOPHYSICA ACTA
BBA
http://www.elsevier.com/locate/bba

Lysolipid incorporation in dipalmitoylphosphatidylcholine bilayer membranes enhances the ion permeability and drug release rates at the membrane phase transition

Jeffrey K. Mills, David Needham *

Department of Mechanical Engineering and Materials Science, Duke University, Durham, NC 27708, USA

Received 17 August 2004; received in revised form 22 August 2005; accepted 23 August 2005
Available online 7 September 2005

Abstract

The enhanced permeability of lipid bilayer membranes at their gel-to-liquid phase transition has been explained using a "bilayer lipid heterogeneity" model, postulating leaky interfacial regions between still solid and melting liquid phases. The addition of lysolipid to dipalmitoylphosphatidylcholine bilayers dramatically enhances the amount of, and speed at which, encapsulated markers or drugs are released at this, already leaky, phase transition through these interfacial regions. To characterize and attempt to determine the mechanism behind lysolipid-generated permeability enhancement, dithionite permeability and doxorubicin release were measured for lysolipid and non-lysolipid, containing membranes. Rapid release of contents from lysolipid-containing membranes appears to occur through lysolipid-stabilized pores rather than a simple enhancement due to increased drug solubility in the bilayer. A dramatic enhancement in the permeability rate constant begins about two degrees below the calorimetric peak of the thermal transition, and extends several degrees past it. The maximum permeability rate constant coincides exactly with this calorimetric peak. Although some lysolipid desorption from liquid state membranes cannot be dismissed, dialyzation above T_m and mass spectrometry analysis indicate lysolipid must, and can, remain in the membrane for the permeability enhancement, presumably in lysolipid stabilized pores in the grain boundary regions of the partially melted solid phase.

Keywords: Liposome; Drug delivery; Vesicle; Thermal-sensitive; Interface; Triggered

1. Introduction

Over 30 years ago, Papahadjopoulos observed that ion permeability through a lipid bilayer membrane showed an anomalous peak as the membrane went through its gel-to-liquid phase transition [1]. At this transition, gel and liquid phases coexist, creating interfacial regions that consist of lipids with large incompatibilities in molecular packing and hydrophobic matching [2]. Since Papahadjopoulos' first discovery, a number of groups have developed models and theories, generally based on two hypotheses, to explain the permeability phenomenon. The first hypothesis, a more continuum approach, relates the increase in permeability to the increase in lateral compressibility of the membrane noted during the phase transition [3,4]. Measurements of the elastic area compressibility of dimyristoylphosphatidylcholine vesicles through the main acyl melting transition region indicate that at the phase transition, the membrane is highly compressible, approximately 5 times more compressible than a completely melted liquid phase membrane and approximately 40 times more compressible than the solid state membrane [5]. Density fluctuations in the bilayer open up cavities in the headgroup region that allow ions to enter and then permeate through the bilayer [3]. The second hypothesis, a more discrete approach at the microstructural level, relates the permeability anomaly to the formation of leaky "interfacial regions" that develop at micrograin boundaries, between gel and liquid domains during the phase transition [2,6–8]. Combining the two, we might hypothesize that the mirograin structure necessitates and discrete model, but that compressibility could indeed be extremely high at melting grain boundaries, allowing for high density fluctuations particularly in these regions and concomitant rearrangement, especially in the presence of a second component.

* Corresponding author. Tel.: +1 919 660 5355; fax: +1 919 660 8963.
E-mail address: d.needham@duke.edu (D. Needham).

0005-2736/$ - see front matter © 2005 Elsevier B.V. All rights reserved.
doi:10.1016/j.bbamem.2005.08.007

Mouritsen and coworkers have developed most of the theories on this second hypothesis, and have proposed a "state of bilayer heterogeneity," describing the bilayer during the transition as a dynamic system of coexisting liquid and solid domains [2,8]. Initially, when the lipid membrane is cooled from the liquid state (say during liposome processing) through its main solidification transition, T_m, solid lipid starts to nucleate in the melt. These nucleates continue to grow and form micrograins of solid lipid in the melt of the liquid membrane. Eventually, as the transition nears completion and the last liquid lipid is transformed, grain boundaries are created between the solidifying domains, and the grains meet at different orientations [8], much the same as occurs in most "traditional" 3-D polycrystalline materials [9]. This nucleation and growth of grains creates a micrograin structure that resembles a soccer ball. Although maybe not as regular a pattern, it is made up of plaques or relatively flat plates of solid lipid, that nevertheless, have to fit on the lipid domain, i.e., a giant lipid vesicle, that can be tens of microns in size or a small (100 nm diameter) spherical liposome. This solid grain structure has been observed in fluorescence microscopy images and freeze fracture electron micrographs of DSPC monolayers on gas microparticles [10] and in transmission electron micrographs of 100 nm gel phase liposomes of the same lipid and lysolipid composition as used in this study containing the anti-cancer drug doxorubicin [11,12]. Crinkled and faceted structures have also been observed using interference contrast microscopy in giant lipid vesicles composed of DMPC when the vesicles were cooled from the liquid phase and solidified under zero tension in the P_β and L_β phases (Needham and Evans, 1987, unpublished results).

When the solidified membrane is heated, melting initiates at these grain boundaries [8], forming interfacial regions between the still solid domains and melting liquid domains. These interfacial regions are composed of lipid chains in intermediate, excited conformational states, resulting in large incompatibilities in molecular packing and hydrophobic matching, and a very "soft" interface [2,8,13]. As found for whole bilayers, compressibility is proportional to permeability, and so it is the "soft" and "leaky" nature of these solid/liquid interfacial regions that leads to the enhanced permeability to ions, drugs and other small molecules that are initially trapped in the liposome interior while the membrane is in its liquid phase, cooled quickly through the transition, remain trapped, and then can leak from the liposome into solute-depleted media as it starts to melt [13]. Most importantly, at the mid point of the transition temperature, the total mismatched area of these interfacial regions reaches a maximum [13], and therefore the permeability also attains a maximum.

This anomalous permeability at the phase transition is enhanced by the inclusion in the bilayer of a second lipid or lipid-like component. The addition of small amounts (10 mol%) of dicaprylPC (diC10) (critical micelle concentration (CMC)=5 μM [14]) to dimyristoylPC (diC14) multilamellar liposomes have also been studied experimentally and modeled using Mouritsen's bilayer heterogeneity model. Incorporation of the shorter dichain lipid decreases the transition temperature of the mixture, from ~24.4 °C to ~21–22 °C [15]. By measuring the permeability of the dithionite ion ($S_2O_4^{-2}$) through multilamellar liposomes, Risbo et al. have determined that the permeability rate at T_m is greater (although a quantitative rate is not provided) in membranes that contain 10 mol% diC10PC, versus pure diC14 vesicles [15]. Mouritsen's theory predicts that the shorter chain lipids partition at the grain boundaries and further disturb molecular packing, thereby increasing the fluctuations and heterogeneity when the interfaces melt which enhances the transition permeability [15].

Our laboratory has developed a thermal-sensitive liposome (lysolipid-containing thermal-sensitive liposome (LTSL)) that takes advantage of the anomalous permeability at T_m due to the melting grain boundaries, resulting in a formulation that releases trapped markers and drug contents at the phase transition but much more quickly (tens of seconds) than in the absence of lysolipid, and in the range clinically attainable by mild hyperthermia (39–42 °C) [16,17]. By incorporating a small amount (10 mol%) of the water-soluble lysolipids (micromolar critical micelle concentration), monopalmitoylphosphatidylcholine (MPPC) or monostearoylphosphatidylcholine (MSPC), into DPPC liposomes prior to cooling from the liquid phase, the peak of the phase transition upon remelting is shifted down slightly from ~41.9 °C to 40.5 °C and 41.3 °C, respectively. Differential scanning calorimetry (DSC) data indicates that, although the addition of lysolipid decreases T_m by more than 1 °C (for MPPC), the breadth of the transition does not change (i.e., does not broaden), strongly suggesting that the identical head group and well-matched acyl chain compositions of MPPC and MSPC mix ideally in the DPPC bilayer [17]. This is further supported by calorimetric and nuclear magnetic resonance data from Van Echteld et al. of mixtures of DPPC and MPPC that also demonstrates ideal mixing of the two components in the solid phase. [18]. More importantly, even though not as fast as at the midpoint of the transition (i.e., at T_m), the onset of release of entrapped contents (6-carboxufluorescein (6-CF)) occurs just above 39 °C, and the MPPC containing LTSLs release over 80% of the 6-CF at 40–41 °C in a few seconds, while pure DPPC liposomes release minimal dye (20%) [17] even after 5 min incubation at their T_m. Similar release results have been obtained for doxorubicin (DOX)-loaded liposomes, and more recent data confirm and extend these findings (Wright, et al, 2005, in preparation). Using the doxorubicin-loaded LTSL formulation, murine studies with a human tumor xenograft model in combination with local hyperthermia (42 °C) showed unprecedented local control (11 out of 11 complete regressions) [16].

Motivated by these preliminary in vitro and pre-clinical studies, the experiments presented here were designed to test two hypotheses regarding the mechanism behind the lysolipid-generated permeability enhancement. The first hypothesis was that whilst trapped in the solid phase in ideal solid solution, upon heating to the transition and even passed it, lysolipid remains in the bilayer and creates permeable defects and enhances drug, aqueous contents marker, and H^+ ion solubility in the bilayer due to increased bilayer free volume. As the bilayer melts and the interfacial regions liquefy, lysolipid already present in the membrane may further enhance the permeability of these regions

due to additional mismatches and lipid heterogeneity as discussed by Risbo examining the effects of adding diC10 PC to diC14 bilayer systems [15]. In addition, lysolipid may be unique and provide actual porous defect structures since its natural self-assembled structures are micelles with a curvature on the order of the bilayer thickness and so its presence in the grain boundaries may help stabilize defects in the membrane as headgroup lined pores. Furthermore, with one less acyl chain per headgroup, (compared to the host di-chain phospholipid) additional free volume could be introduced that may simply increase solubility to the permeant species. The second hypothesis is that, again, whilst trapped in the solid phase, the water-soluble lysolipid (critical micelle concentration (CMC) of MPPC=4–7 μM [19,20], CMC of MSPC=4 μM [19]) may desorb from the bilayer, entering the external media that is devoid of lysolipid, leaving behind vacancy defects in the partially melted solid/liquid interfacial regions through which small molecules could pass. This "washout" of lysolipid has been noted in micropipette experiments where single liquid phase giant vesicles (stearoyloleoylphosphatidylcholine (SOPC)) were bathed in a solution of monooleoylPC (MOPC) [21,22]. After initial incorporation of about 6 mol% of lysolipid in the membrane, while the membrane remained intact, the lysolipid quickly dissolved out of the membrane when bathed in a diluting medium [21,22]. It is important to note though, that in these experiments the uptake was only into the outer monolayer (transport by flip-flop of the lysolipid to the inner bilayer leaflet takes much longer, by a factor of about 100, than the adsorption from and desorption into the aqueous phase) and therefore desorption was from the outer monolayer before significant amounts of lysolipid had been allowed to cross the bilayer and partition into the inner monolayer. In the liposome formulations tested here, the lysolipid is introduced into the mixture from the beginning of lipid preparation and is necessarily partitioned almost equally between the two halves of the bilayer. Whether the lysolipid is therefore free to desorb fully from both halves of the bilayer (as opposed to just the outer monolayer) is of interest to test.

In order to distinguish between the two mechanisms listed above, and to more comprehensively characterize the nature of this enhanced membrane permeability, we have measured the permeability rates of two unique molecules through lysolipid-containing membranes, as well as other pure lipid bilayers, under different conditions. To eliminate the apparently partial contents release initially noted with 6-Carboxyfluorescein in some of our previous work [17], the dithionite ion ($S_2O_4^{-2}$) was selected as a single, small molecule that does not form molecular aggregates, and therefore its permeability should not be limited by possible defect size selectivity. Measurements of the release rate of DOX through the two lysolipid formulations and pure DPPC membranes have also been made. The results from this investigation indicate that lysolipid does not readily desorb from the membrane upon heating to, and through the transition, and supports the presence of lysolipid-stabilized pores in the membranes, probably at melting grain boundaries, that facilitate the rapid release of contents from the lysolipid thermal-sensitive liposome formulations upon heating to the phase transition region.

2. Materials and methods

2.1. Materials

Dipalmitoylphosphatidylcholine (DPPC, T_m=41.5–41.9 °C [23]), monopalmitoylphosphatidylcholine (MPPC), monostearoylphosphatidylcholine (MSPC), palmitoyloleoylphosphatidylcholine (POPC, T_m=−2 °C [23]) and distearoyl-phosphatidylethanolamine-poly(ethylene glycol)-2000 (DSPE-PEG (2000 molecular weight poly(ethylene glycol)) were purchased from Avanti Polar Lipids, Inc., AL and used without further purification. N-(7-nitrobenz-2-oxa-1,3-diazol-4-yl)-1,2-dihexadecanoyl-*sn*-glycero-3-phosphoethanolamine, triethylammonium salt (NBD-PE) was obtained from Molecular Probes, Inc. Sodium Hydrosulfite ($Na_2S_2O_4$), TRIZMA base, doxorubicin (DOX), citric acid and Triton X-100 were obtained from Sigma Chemical Co. Sodium chloride, and sucrose were purchased from Mallinckrodt, Inc. Sephadex G-50 was obtained from Amersham Pharmacia Biotech.

2.2. Dithionite permeability: background and development of the absorbance assay

Several groups have measured the permeability of anions and cations through lipid vesicle bilayers. Most of the methods utilize ion-sensing electrodes or radiolabeled ions that require very specialized equipment and laboratory environments [1,24,25]. In this report, we measure the permeability of the dithionite ion ($S_2O_4^{2-}$, pK_a's=0.35, 2.45 [26]) through liposome membranes using simple spectrophotometric absorbance measurements.

In aqueous solution, the dithionite ion is in equilibrium with the SO_2^- radical, a reaction intermediate in the nitro reduction of N-(7-nitro-2,1,3-benzoxadiazol) (NBD) to its corresponding amine [27]. This reduction results in the irreversible quenching of NBD fluorescence and virtually eliminates the absorbance peak of NBD at 465 nm [28]. A number of groups have used dithionite quenching of NBD fluorescence to measure lipid distribution [29,30] and flip-flop [31]. Fluorescence quenching has also been used to measure permeability through multilamellar vesicles [15,32] and single bilayer vesicle membranes [33]. There are several concerns with the fluorescence method, however, that can complicate permeability measurements. First, continuous excitation of the fluorophore causes it to photobleach, which can be mistaken for the NBD-dithionite quenching reaction. Secondly, it is unclear whether or not self-quenching occurs between the labeled lipids (expected at relatively high fluorescent lipid concentrations which nevertheless can be in the few mol% range), especially if and when they come in close proximity to each other at the bilayer surface, as in grain boundaries (observations from this work). In addition to these concerns, the use of multilamellar vesicles does not accurately model the single bilayer, ~100-nm diameter, extruded vesicles that are generally used in clinical applications. In the experiments presented here, the permeability was measured through extruded, unilamellar vesicles, using an absorbance decay assay, which eliminated any photobleaching or self-quenching concerns, and also allowed for the determination of accurate temperature-dependent permeability rate constants on clinically relevant samples.

Incorporation of 1 mol% of NBD head group labeled lipid into large, unilamellar vesicles (LUV, ~100 nm in diameter) results in a slightly asymmetrically labeled bilayer [30], with a detectable 54% of the NBD molecules residing on the outer monolayer and 46% residing on the inner monolayer due to curvature restrictions (see results). The addition of dithionite to the outside of the liposomes causes an immediate reaction with the NBD molecules on the exterior monolayer (complete reaction within about 10–20 s). Permeation of the $S_2O_4^{-2}$ ion or SO_2^- radical through the bilayer results in a subsequent reaction with the inner monolayer at a rate of ~0.25% labeled-lipid reacted/minute (i.e., permeation and reaction at this rate; dioleoyl-PC vesicles at room temperature) [28]. Bilayer permeability is therefore the rate limiting factor in the reaction. By monitoring the optical absorbance at 465 nm, measurements of the temperature-dependent dithionite permeability rate through DPPC and two LTSL bilayer membranes (DPPC:MPPC and DPPC:MSPC) were made. Although permeability rate constants are temperature and composition dependent, all membranes reached

100% reacted NBD over some time scale, eliminating any "pseudoequilibrium" temperature discrepancies that were previously noted in our measurements of 6-CF release with similar lipid compositions [17]. Permeability through palmitoyloleoylphosphatidylcholine (POPC, T_m ~2 °C) vesicles was also examined as a measure of the temperature-dependent permeability of liquid state membranes throughout the temperature range studied as a non-phase transition lipid control.

2.3. Liposome preparation for dithionite permeability measurements

Four liposome compositions based on DPPC were examined using the dithionite permeability assay (all percentages indicate mol% of the minor component(s)) DPPC:DSPE-PEG(4%), POPC:DSPE-PEG(4%); and LTSL formulations DPPC:MPPC(10%):DSPE-PEG(4%) and DPPC:MSPC(10%): DSPE-PEG(4%). Two sets of lipid samples were required for each measurement. They were identical in composition, except that the "Blank" sample (used as a reference for the spectrophotometer) did not contain labeled lipid, while the other sample, "NBD-labeled," contained 1 mol% NBD-PE. For each set, lipids were co-dissolved in chloroform and then dried onto a round bottom flask using a rotovapor. Each film was hydrated with 1.5 ml of a solution (~pH 7) of 100 mM NaCl with 709 mM sucrose (20 mg/ml final lipid concentration). The salt provided ion screening, while the sucrose was added to increase the solution osmolarity to ~900 mOsm. This elevated osmolarity ensured that when 30 mM dithionite ions were added, the increase in external solution osmolarity relative to inside the liposomes was only ~6% and all but eliminated osmotic pressure across the membranes. (Note: because the permeability measurement is due to dithionite crossing the bilayer from outside to inside, this initial osmotic gradient is not responsible for the observed permeability enhancement, as it may be if the permeant species was trapped inside and moved out down an osmotic flow.) In the case of the lysolipid temperature-sensitive formulations, the NaCl/Sucrose buffer for hydration also contained 1 μM of the appropriate lysolipid (MPPC or MSPC) to provide an equilibrating amount of lysolipid in solution during self-assembly. The liposomes were then extruded using a Lipex Biomembranes Thermobarrel Extruder (Lipex Biomembranes, Vancouver, BC) through two, 100 nm polycarbonate membrane filters (Poretics) so as to yield a homogeneous sample of unilamellar lipid vesicles. For both hydration and extrusion of liposomes, the temperature of the sample was maintained above T_m at 45–48 °C with a circulating water bath to ensure that the liposomes were liquid phase and the lipid composition was well mixed in the bilayer.

Following extrusion, the liposomes were cycled five times through their transition temperature, allowing the sample to equilibrate for 5 min above (~48 °C) and below (10 °C) T_m. This cycling ensured that vesicles that may initially rupture due to the ~25% reduction in bilayer area during the first lipid-freezing cycle [34] can re-anneal into intact liposomes with minimal tension in their membranes upon re-heating to the liquid phase and so reseal. Finally, after cooling the liposomes to room temperature and their solid state, (final cooling rate ~40 °C/min), they were passed through a Sephadex G-50 column, pre-equilibrated with the NaCl/Sucrose buffer, to remove free lysolipid.

2.4. Differential scanning calorimetry

In order to measure the calorimetric phase transition profiles, including the transition temperatures of the various samples, all lipid components were first co-dissolved in chloroform at the appropriate ratios. A lipid solution of each of the four compositions (excluding POPC-no phase transition in the temperature range of interest) was prepared at a concentration of approximately 20 mg of total lipid per ml of chloroform. 250 μl (5 mg total lipid weight) of this mixture was then dried on the bottom of a glass vial under a stream of nitrogen and stored under vacuum overnight at room temperature. The next day, the lipid film was scraped off the bottom of the vial and 1 mg of the film scrapings was placed directly into the base of an aluminum Perkin-Elmer DSC pan. 10 μl of DI water was then added to the lipid sample and the sample pan was sealed using the aluminum top and a Perkin-Elmer Sample Pan Crimper Press. The entire sample pan was then heated to 60 °C for 1 h to fully hydrate the sample. The samples were then thermally scanned from 30 to 50 °C at a rate of 0.2 °C/min.

2.5. Absorbance measurements

After column filtration, both "blank" and "NBD-labeled" liposomes were diluted in NaCl/Sucrose buffer to a final lipid concentration of 3 mM. Absorbance measurements were made using a Shimadzu UV-1601 Spectrophotometer. This instrument uses a dual cuvette system, where the "sample" cuvette (NBD-labeled sample) is always measured relative to a "reference" cuvette. Initially, both cuvettes were filled with 1 ml of "blank" liposomes that did not contain NBD-labeled lipid. Both "sample" and "reference" cuvettes were equilibrated to the proper recording temperature with the use of a circulating water bath connected to the spectrophotometer's water circulation system. The "sample" cuvette was stirred using an Instech® stirring system that fits on the top of the cuvette and uses a short stirring rod to agitate the solution. The temperature was monitored with a small thermocouple wire inserted into the cuvette. After 10 min of equilibration, the spectrophotometer was "zeroed" at 465 nm, i.e., any absorbance at this wavelength was subtracted from the "sample" reading (normally on the order of a few tenths of a percent). The "sample" cuvette was washed and then filled with 1 ml of "NBD-labeled" liposome solution, while the "reference" cuvette and solution were left in the instrument.

The "sample" was then equilibrated to the appropriate temperature for 10 min with constant stirring. After 10 min, absorbance readings at 465 nm were started, with the instrument programmed to automatically record measurements every 10 s. These readings were always within 1% of each other, yielding a stable absorbance trace. After 2 min, 30 μl of 1 M Dithionite ions was added to both cuvettes (30 mM total ions). 1 M Dithionite solution was prepared from Sodium Hydrosulfite ($Na_2S_2O_4$) in 1 M TRIZMA buffer. Addition of ions to both cuvettes insured that any decrease in absorbance was due to dithionite–NBD reaction and not simply to dilution of the "sample" volume. The stirring mechanism was replaced and the absorbance of the "sample" was recorded for a total of 30 min, with measurements automatically recorded every 10 s. After 30 min, 20 μl of 10% TRITON X-100 was added to both cuvettes. (TRITON X-100 does not alter the absorbance signal at 465 nm.) After 5 min, to allow for complete liposome lysis and exposure of all unreacted lipid, a final absorbance reading was made. This reading corresponded to 100% reacted NBD molecules (additional dithionite ions did not reduce this final value).

The addition of dithionite to the outside of the liposomes resulted in an immediate reaction of the NBD molecules on the exterior monolayer (complete reaction within about 10–20 s). Permeation of the $S_2O_4^{-2}$ ion or SO_2^- radical through the bilayer resulted in a subsequent reaction with the inner monolayer [28]. By monitoring the optical absorbance at 465 nm, measurements of the temperature-dependent rate constant at which dithionite ions cross the bilayer membranes were made.

2.6. Lysolipid enhancement mechanism

The experiments outlined below were designed to determine whether lysolipid desorption from the bilayer was responsible for the permeability enhancement, or if it was the presence of the single chain lipid, remaining in the membrane and creating in situ defects, possibly at grain boundary regions, that accounted for the increase in transmembrane transport over and above the anomalous permeability at the phase transition of the pure lipid.

In the first experiment, dithionite permeability measurements were made following dialysis of the liposomes to remove any desorbing lysolipid as follows. Liposomes were prepared as outlined above. Following column filtration, 1 ml of the NBD labeled sample was placed in a Pierce® "Slide-A-Lyzer" dialysis chamber (10,000 MW cutoff). This chamber was dialyzed at 45–48 °C against 400 ml of the NaCl/Sucrose buffer. At this elevated temperature, the liposome membranes are in a completely liquid phase and therefore should allow the water-soluble lysolipid every chance to desorb and enter the external medium [21,35]. After dialysis for 24 h, the external buffer was exchanged for another 400 ml of NaCl/Sucrose and the sample was dialyzed for another 24 hrs at 45–48 °C. Initially, the lysolipid concentration in the membrane was equivalent to ~0.3 mM in the total solution volume. After

the first dialysis, the concentration (assuming all of the desorbing lysolipid had reached equilibrium between the membrane and solution) would be ~100 μM, still above the critical micelle concentration (CMC) of MPPC of ~4–7 μM [19,20]. After the second dialysis cycle, however, the concentration, if all the lysolipid desorbed, would be approximately 38 nM, well below the CMC and therefore expected to be present only as single monomers in solution. Following the second overnight incubation, the vesicles were removed from the dialysis chamber, cooled to room temperature, and the dithionite permeability experiments were performed as before.

Dithionite permeability measurements were also made using vesicles that did not initially contain 10 mol% MPPC in the lipid film, but instead, the lysolipid was added to the outside of preformed DPPC liposomes. DPPC:DSPE-PEG(4%):NBD(1%) vesicles were hydrated and extruded as above and allowed to equilibrate for 10 min in the spectrophotometer cuvette at the appropriate temperature. The equivalent of 10 mol% MPPC was then added to the external volume (bringing the solution to 0.3 mM MPPC) and allowed to equilibrate with the vesicles for 10 min at the test temperature The dithionite-absorbance decay assay was then carried out as before. These experiments were used to determine whether MPPC initially outside the membranes caused the same permeability enhancement as if it were incorporated during the hydration process, i.e., its presence in the membrane was required for the enhancement.

Thin Layer Chromatography (TLC) and Proton Nuclear Magnetic Resonance (NMR) analysis were performed to clarify whether lysolipid was remaining in the membrane, or desorbing out of the liposomes, during the dialysis procedure. For TLC analysis, the following three samples were prepared: 30 mg of DPPC:DSPE-PEG(2000) (4%), 30 mg of DPPC:MPPC(10%):DSPE-PEG(2000) (4%) and 2.03 mg (i.e. equivalent to 10 mol%) MPPC. Each sample was hydrated with 1 ml NaCl/Sucrose, extruded, and then dialyzed for 48 h as described above. A phase separation procedure was then used to remove the water from the samples. 100 μl of each sample were placed in an Eppendorf tube and 375 μl of chloroform/methanol (1:2 volume ratio) was added to generate a monophase. The solutions were vortexed, and 125 μL of chloroform was added, and the solutions vortexed again. 125 μl of DI water was added, resulting in a phase separation. The samples were then spun down in an Eppendorf tube, using a microcentrifuge at 9000 rpm for 1 min. This produced a two-phase sample, with an upper water phase and a bottom organic layer containing the lipids. The top water layer was removed and the bottom layer dried down under a stream of nitrogen and then dried fully under vacuum overnight. 181 ml of chloroform was added to each sample to completely solubilize the lipid for spotting.

10 μl (~150 nmol of lipid) of each of these solutions were spotted on a silica TLC plate using a Hamilton Syringe. The plate was then placed in a glass development chamber containing ~200 ml of the solvent mixture chloroform/methanol/DI H_2O (65:25:4, volume ratios). The top of the chamber was sealed with vacuum grease and the plate was run for approximately 1 h, or until the solvent reached a few centimeters from the top of the TLC plate. The plate was removed from the chamber and allowed to dry completely before developing with iodine crystals.

Proton Nuclear Magnetic Resonance Spectroscopy (NMR) measurements were performed as follows. A 100 mg sample of DPPC:MPPC(10%):DSPE-PEG(2000) (4%) (no NBD) was prepared as above, but here, 2 ml D_2O was used to hydrate the sample rather than NaCl/Sucrose buffer. Following extrusion, 1 ml of this sample was placed in a slide-a-lyzer set-up and dialyzed for 48 h at 45–48 °C against 50 ml of D_2O. Following the incubation, the dialyzed sample and a sample of the dialysate (external D_2O) were removed for analysis. Two control samples were also analyzed; a non-dialyzed DPPC:MPPC(10%):DSPE-PEG(2000) (4%) sample and a control sample of MPPC in D_2O. This control MPPC sample was 0.27 mM, a concentration equivalent to MPPC in the external dialysate assuming that all of the MPPC desorbed out of the vesicles. The MPPC control and dialysate sample were analyzed at room temperature. Both of the DPPC:MPPC(10%):PEG(4%) samples were analyzed at 50 °C (above T_m) to enhance the rotation and proton signals from the lipids.

2.7. Micropipette manipulation

Just as had been done for DMPC and SOPC/POPE vesicles previously [34,36] we carried out micropipette studies to observe, for giant lipid vesicles (~30 μm diameter), the lipid vesicle membrane area changes (equivalent to the cumulated DPPC area per molecule changes) that accompany the phase transition in the LTSL formulation, and to check to see if the vesicles stayed intact as they were taken through the gel/liquid phase transition temperature during a heating scan and cooling scan. Vesicles for micromanipulation were prepared by hydrating ~1 mg of DPPC:MPPC(10%):DSPE-PEG(4%) lipid dried onto a Telfon disk with 15 ml of 200 mM sucrose [37]. The vesicles were then incubated for 3 h at 45 °C. They were then diluted ~5 μl:1000 μl in 200 mM glucose and placed into a temperature-controlled micromanipulation chamber containing 200 mM glucose [38,39]. Single, giant unilamellar vesicles were selected from the bottom of the chamber and held in a ~10 um diameter micropipette with a very low suction pressure (20–30 dyn/cm^2) just to keep the vesicles from floating away from the pipette [34,40]. The vesicles were then cycled five times through their transition temperature of 40.5 °C (starting at ~35 and ending at ~42 °C, holding for several minutes at each end temperature).

2.8. Doxorubicin loading

Doxorubicin (DOX) was loaded into the liposomes using the pH gradient loading method described initially by Mayer et al. [41] and later by Madden et al. [42] with slight modifications (loading times and incubation temperatures). Thirty mg lipid films (DPPC:DSPE-PEG(4%), DPPC:MPPC(10%):DSPE-PEG(4%) and DPPC:MSPC(10%):DSPE-PEG(4%)) were hydrated with 3 ml (10 mg/ml lipid) of 300 mM pH 4. 0 Citric Acid buffer containing 1 μM of the appropriate lysolipid for the LTSL formulations. The liposomes were then extruded through two 100-nm filters. This lipid suspension was cooled to room temperature and maintained below its transition temperature until drug loading. In order to establish the pH gradient as described in Madden et al. [42], the liposomes were passed through two consecutive, different Sephadex G-50 mini size exclusion columns. Rather than using DI water to hydrate the gel beads for the columns, 20 mM HEPES (Sigma) buffer at pH 7.4 was used so that the external pH 4.0 citrate buffer was exchanged for the pH 7.4 HEPES buffer in the beads, while maintaining the pH 4.0 liposome interior. Doxorubicin was prepared at 5 mg/ml in saline (0.8 g NaCl/100 ml in DI water) and added to the liposome suspension at a 10:0.5, lipid/drug, weight ratio. The liposomes and DOX were then incubated together.

For the pure DPPC liposomes, >95% drug loading was achieved reproducibly by incubating at 60 °C for 10 min [43]. If the LTSL formulations are heated above T_m to maximize drug loading, within a few minutes at T_m, the pH gradient was lost (Ickenstein and Anyarambhatla unpublished results). Because of the enhanced transition permeability, the citrate buffer also appears to leak out of the liposome interior as doxorubicin is noted to gel in the external solution if the temperature is raised to the transition region, not having necessarily gone above T_m, with DOX present in the external medium. This implies that the pH gradient can readily dissipate because of the acute permeability of this temperature-sensitive formulation, and as we will show in the data, this can occur on the lower shoulder of the calorimetry profile, 1–2 degrees below the mid point of the transition signified by T_m. Therefore, a method of loading the drug below its transition temperature was developed. The pH gradient is established in the same manner as above, but incubation with drug was carried out at room temperature (23–25 °C) overnight (20–24 hrs) for the DPPC:MPPC (10%) formulation, and at 37 °C for 20 min for the DPPC:MSPC (10%) formulation. Even though the membranes are in a gel phase, the presence of the lysolipid increases the permeation, maybe by increasing solubility of DOX through the membrane, so that drug is able to cross into the interior of the liposome (see Results for a more complete description). By maintaining the temperature well below the threshold for substantial hydrogen ion permeability, and loading at a drug to lipid ratio of 0.5:1 (w/w) (approximately 0.4:1 mol/mol), greater than 98% drug loading was achieved.

To determine the amount of drug loaded, a simple fluorescence assay was used based upon Doxorubicin's self-quenching properties [44]. This characteristic can be used to measure both release of drug, as well as percent loading. Following the drug incubation step, the vesicles were cooled to room temperature and then passed through a Sephadex G-50 (prepared in HEPES) mini-column to remove any unencapsulated drug. To measure the encapsulation efficiency, 5 μl of liposome-loaded solution (pre-column) was added to 1 ml HEPES buffer along with 5 μl of 10% TX-100 to lyse the vesicles and release

all of the drug, and a fluorescence reading was made using an excitation wavelength of 470 nm and an emission wavelength of 555 nm. A second 5-μl sample (post-column) was then measured in the same manner. Percent encapsulation was determined as follows:

$$\text{Percent Encapsulation} = FL_{TX}(\text{post column})/FL_{TX}(\text{pre column})*100 \quad (1)$$

2.9. Doxorubicin release measurements

The most ideal method to measure the temperature-dependent drug release from a liposome sample would be to monitor a single sample heated to the temperature of interest over a set time interval. Unfortunately, in the case of DOX release from liposomes, this was not possible. In general, Doxorubicin is an excellent choice for initial drug encapsulation and release measurements due to its well-established loading methods and the fluorescence-dequenching assay described above. However, constant excitation of the drug causes substantial photobleaching, and therefore it was not possible to expose the same sample to several fluorescence measurements in order to obtain time-dependent drug release data. To alleviate this concern, we worked with individual samples for each temperature and time, and the following method was used.

Small (12 × 75 mm) glass test tubes (35 total tubes) were filled with 1 ml of HEPES, pH 7.4 buffer at room temperature (same buffer as was used during the drug loading procedure). To each test tube, 5 μl of DOX-loaded liposomes was added and mixed gently by swirling. All of the test tubes were placed into a test tube rack, and the entire rack was submerged into a circulating water bath equilibrated to the temperature of interest so that the solution in the tubes was completely submerged below the level of the water, but the tops of the tubes were not in contact with the water.

For the first 5 min, starting at time zero, one test tube was removed every 20 s. Immediately upon removal, the test tubes were placed into an ice water bath to quickly cool them below T_m (less than 1 s) and stop any subsequent drug release. Drug release at the experimental temperature was monitored over 30 min with a single tube removed every 60 s (5–18 min) and then every 120 s (20–30 min). In this manner, every test tube gave a single time point, all the way up to the last 30-min time point. When the last test tube was removed, each sample was read separately by placing the tube's entire 1 ml into a quartz cuvette and recording the fluorescence as above (Fl_t). Six random samples were then chosen, lysed with 5 μl of 10% TX-100 and a final fluorescence recording was made. These six readings were then averaged for a final "100% Released" value (Fl_{TX}). Percent of drug release was then calculated, where, Fl_{t0} was the fluorescence of the zero time point sample.

$$\text{Percent Release} = [(Fl_t - Fl_{t0})/(Fl_{TX} - Fl_{t0})]*100 \quad (2)$$

Percent release from Eq. (2) was converted into moles of drug released as follows. 100 nm liposomes have an entrapped volume of approximately 1 μl/μmol of lipid [45]. Based upon the initial amount of lipid, and assuming that each liposome was unilamellar, the total encapsulating volume was estimated. Since the amount of drug added to the liposomes, and the loading efficiency were both known, it was straightforward then to calculate the amount of drug, in moles, encapsulated and then released. For the procedure described above using 20 mg of lipid and 1 mg of drug loaded at 98% efficiency:

Total volume of liposomes loaded = 27.2 μl;
Concentration of drug loaded = 62.4 mM;
Total number of moles in 5 μl aliquot = 3.86 nmol.

3. Results

3.1. Dithionite permeability

The dithionite permeability experiment gave a measure of the amount of dithionite that crossed the membranes of the liposomes in the sample as a function of temperature, since dithionite rapidly quenches the NBD fluorescence and absorbance (measured at 465 nm) of the labeled liposomes on the outside monolayer, and on the inside if the membranes are permeable. To allow for comparisons between the various compositions, readings from the absorbance spectrophotometer were converted to relative absorbance values as follows. Prior to the addition of dithionite, the initial 2 min of steady state absorbance readings for the unreacted liposome sample were averaged (twelve total readings), resulting in a value that corresponded to "100% unreacted NBD" (Abs_{Init}). The addition of dithionite caused the absorbance to quickly drop (within 20 s) as all of the NBD molecules on the outside monolayers of the liposomes reacted (as an example, see Fig. 1, sample at 30 °C). Any subsequent decay of the absorbance signal (Abs_{Dith}) was due to permeation of the dithionite ion through the lipid membrane and reaction with NBD molecules on the inner monolayer. After 30 min, the addition of TX-100 destroyed all of the vesicles, allowing dithionite to react with all NBD molecules, and a final reading was made (Abs_{TX}). This value was never zero due to some residual absorbance signal, but was only ever a few percent of the initial absorbance. Data collected after the addition of dithionite was corrected by subtracting this residual "100% reacted" value. Dividing all of the data by the 100% unreacted NBD (ABS_{init}) value gave relative absorbance readings as follows:

$$\text{Relative Absorbance} = \frac{Abs_{Dith} - Abs_{TX}}{Abs_{Init}} \quad (3)$$

It is important to note that the absorbance decay noted in Figs. 1 and 2 is not simply a time-dependent dithionite-NBD reaction. The reaction between free NBD-labeled lipids and dithionite ions occurs within ~10–20 s in the stirred sample, regardless of the temperature examined (as measured here and also noted in [29]). In addition, the number of dithionite ions added to the cuvette outnumbers the NDB molecules by 1000:1, ensuring that the reaction does not significantly deplete the pool of ions.

Dithionite permeability through the DPPC:DSPE-PEG(4%) membranes is represented in Fig. 1 as a plot of Relative Absorbance at 465 nm versus Time in minutes for five temperatures in the examined range (30 °C–48 °C). Data points and error bars represent the mean and standard deviation

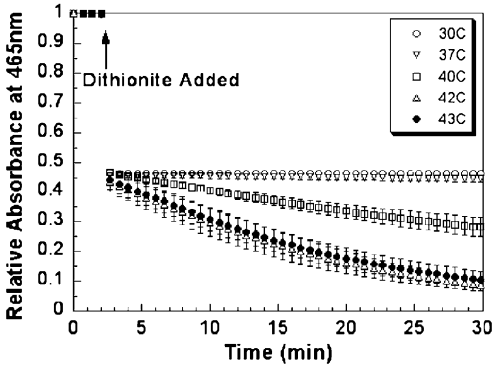

Fig. 1. Dithionite permeability through DPPC:DSPE-PEG(2000) (4%) membranes. Relative Absorbance at 465 nm vs. Time (min) is shown for five temperatures in the examined range. Data points and error bars represent the mean and standard deviation respectively of three separate experiments.

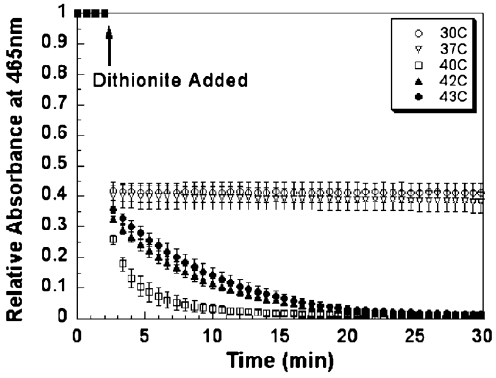

Fig. 2. Dithionite permeability through DPPC:MPPC(10%):DSPE-PEG(2000) (4%) membranes. Relative Absorbance at 465 nm vs. Time (min) is shown for five temperatures in the examined range. Data points and error bars represent the mean and standard deviation, respectively, of three separate experiments.

of three separate experiments at each temperature. Only every fourth data point is shown to help with symbol identification. For the first 2 min of the unreacted sample, the relative absorbance remains steady at "1" for all traces. Following the addition of dithionite at 2 min, the relative absorbance quickly drops to ~0.46 (the 130-s time point is not shown for all traces as it often took just slightly longer than 10 s to add the dithionite ion to both cuvettes). This value of 0.46 corresponds to 46% remaining NBD molecules that have not reacted on the inner monolayer of the liposomes in the sample. Any subsequent loss of the absorbance signal is due to dithionite ions crossing the bilayer and reacting with the NBD lipids on the inner monolayer. Vesicle diameter was measured to be 125±13 nm by Photon Correlation Spectroscopy using a Coulter N4 Plus Submicron Particle Sizer. The small curvature of a 125-nm diameter vesicle (with its 4 nm thick membrane) makes the surface area of the outer monolayer slightly larger by a ratio of 54:46. The NBD lipids partition evenly, but since there are overall less lipids in the inner monolayer than the outer, the total absorbance changes reflect these relative inside to outside absolute numbers of lipids at ~54%:46% outer/inner. The ability to detect these ratios confirmed the technique as being an accurate representation of the lipid amounts in the outer and inner membrane compared with previous fluorescent lipid concentration measurements, which in turn then reflects permeability as the lipid absorbance is altered by dithionite transport.

Thus, in Fig. 1 at 30 °C, there is no measurable dithionite ion permeability through the DPPC membranes, as the absorbance readings remain stable at 0.46 over the 30-min time course. At the higher temperature of 37 °C (for a new sample), a slow decay in the absorbance trace with time is noted (~4% over 30 min), indicating that ions are slowly permeating through the membrane. The absorbance curve at 40 °C shows even faster absorbance decay and permeability, while at 42 °C (the transition temperature of DPPC, as determined from DSC measurements) the absorbance drops fairly quickly with time. The absorbance trace at 43 °C shows a slightly slower rate of decay indicating a peak in permeability around 42 °C. In all cases, where permeability is noted, if the experiment is followed for longer times (hours to days), the curves will effectively reach 0 (less than 0.009) relative absorbance demonstrating complete access by dithionite to the interior-liposome lipids.

Fig. 2 shows a similar plot of relative absorbance at 465 nm versus time for the DPPC:MPPC(10%):DSPE-PEG(4%) membranes, but this time the decay in absorbance is much more rapid at T_m. At 30 °C, the absorbance remains steady at 0.42. Although a minor effect, it appears that the addition of 10 mol% MPPC creates a slight preferential distribution of NBD lipid to the outer monolayer from the expected 54% to 58% and concomitantly reduces the amount of lipid in the inner monolayer from 46% to 42%. Liposome diameters were comparable DPPC controls. As with DPPC, the permeability of the DPPC:MPPC(10%) membranes increases only slightly when the temperature is raised to 37 °C. As the temperature is raised to 40 °C, very near to the transition temperature for DPPC:MPPC(10%) (~40.5 °C from DSC measurements, i.e., slightly lower than for pure DPPC), the permeability increases dramatically, as the absorbance drops to less than 40% remaining NBD absorbance within in the first 60 s following the addition of dithionite, to only 5% remaining within 6 min, and falling to ~1% remaining by 15 min. Increasing the temperature for DPPC:MPPC(10%), traces at 42 and 43 °C show slower absorbance decay than at T_m, but faster than DPPC at the same temperatures, illustrating, again, a permeability maximum at T_m.

In order to obtain a quantitative measure of the ion permeability, Fig. 3 shows the method used to determine the temperature-dependent ion permeability rates. Data and fits are shown for three DPPC traces as an example. All compositions and temperatures were analyzed in the same manner. Only data collected after the addition of dithionite (>2 min, i.e., after the outer monolayer reacted) was fit to determine the permeability rate constants. The following equation was fitted to the data using the Curve Fit feature of KaleidaGraph®.

$$\text{Relative Absorbance} = m1^{*}\exp[-m2^{*}(t)] \quad (4)$$

Here, $m1$ and $m2$ are constants, and t is time in minutes. $m1$ is the intercept of the best fit line with the time axis, and therefore represents the amount of relative absorbance remaining after the outside monolayer has been reacted, i.e. ~0.46 (or 0.42 as in the case of the Lysolipid-containing samples). The constant, $m2$, represents the rate constant of the absorbance decay. In all cases, the correlation coefficient (R) was greater than 0.95 where exponential decay was noted (i.e. greater than 30 °C). In the example in Fig. 3 for DPPC, the values for $m1$ are all fairly close to the expected 0.46, and $m2$ increases from ~0.0012 at 30 °C to ~0.019 at 40 °C, to ~0.058 at 42 °C. The same curve fitting was performed on all the absorbance data for all membranes studied, and in all cases, the correlation between the curve fit and data for all temperatures greater than 30 °C was greater than 0.95 showing that the dithionite ion transport across the membrane, and its binding to the inner NBD lipids, was an exponential process. Given that binding is not the rate determining step [29], it is bilayer transport that is being measured and is an exponential.

Fig. 4 is a compilation plot of the permeability rate constants ($m2$, in units of 1/min) for pure DPPC:DSPE-PEG(2000)

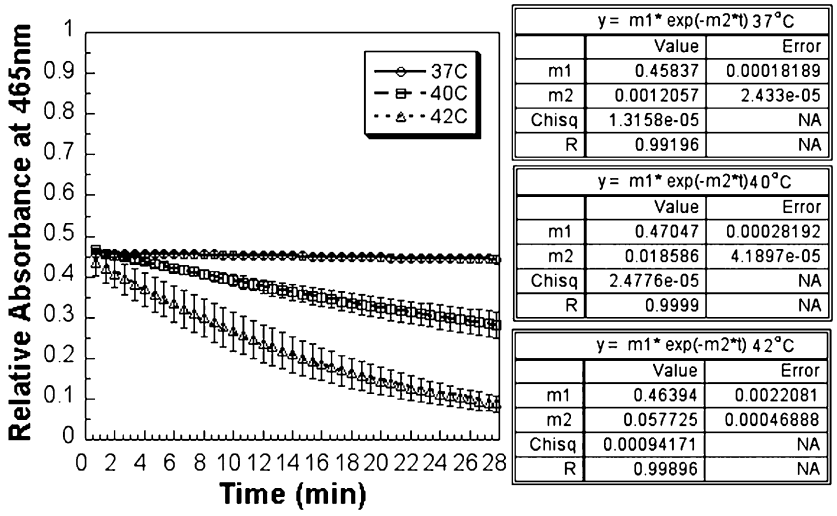

y = m1* exp(-m2*t) 37°C		
	Value	Error
m1	0.45837	0.00018189
m2	0.0012057	2.433e-05
Chisq	1.3158e-05	NA
R	0.99196	NA

y = m1* exp(-m2*t) 40°C		
	Value	Error
m1	0.47047	0.00028192
m2	0.018586	4.1897e-05
Chisq	2.4776e-05	NA
R	0.9999	NA

y = m1* exp(-m2*t) 42°C		
	Value	Error
m1	0.46394	0.0022081
m2	0.057725	0.00046888
Chisq	0.00094171	NA
R	0.99896	NA

Fig. 3. Method used to determine dithionite ion permeability rate constants. DPPC:DSPE-PEG (2000) (4%) relative absorbance data vs. time collected after the addition of dithionite (i.e., 2 min and outer monolayer reacted) were fit using an exponential: $y = m1 \times \exp(-m2 \times t)$. Here, $m1$ represents the intercept and $m2$ (1/min) the temperature-dependent rate constant. In all cases where absorbance decay was observed, correlation was greater than 0.95.

(4%), POPC:DSPE-PEG(2000)(4%), DPPC:MPPC(10%): DSPE-PEG(2000) (4%) and DPPC:MSPC(10%):DSPE-PEG(2000) (4%) through the temperature range, 30–52 °C. The lines joining the data are shown simply to aid the eye. The permeability rate constants for DPPC from 30–37 °C are very slow, less than 0.0013/min, and then begin to increase near 39 °C and reach a local maximum of 0.058/min at ~42 °C (T_m). The rate constants then drop below this local maximum when the temperature is increased to 42.5 °C, remain lower through ~44 °C, and then increase above the anomalous permeability peak at T_m, if the temperature is raised above 45 °C.

Permeability rate constants for POPC shown in Fig. 4 represent dithionite ion permeation through an intact bilayer membrane that is in its liquid crystalline phase over the entire temperature range. A steady increase in dithionite permeability rate constants occur with increasing temperature, but no local maximum is noted, because there is no phase transition over the temperature range. It is interesting to note that the DPPC curve becomes coincident with the liquid phase POPC curve at temperatures above T_m, i.e., when both membranes are in their liquid phase, and that the anomalous peak in permeability at the DPPC transition is only slightly higher than this liquid phase lipid at the same temperature.

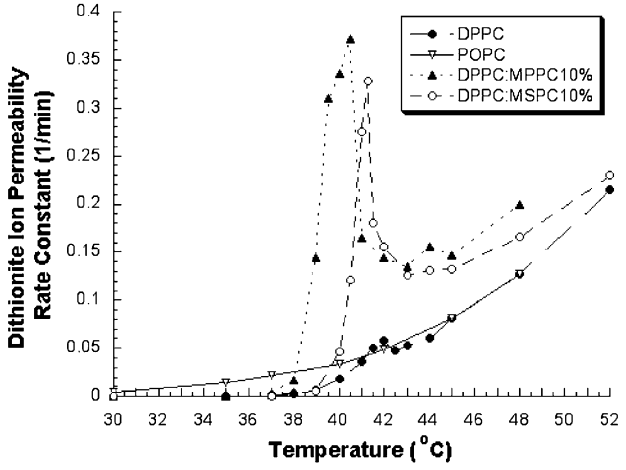

Fig. 4. Compilation of dithionite ion permeability rate constants (1/min). Rate constants are shown for DPPC:DSPE-PEG(2000) (4%), DPPC:MPPC(10%): DSPE-PEG(2000) (4%), DPPC:MSPC(10%):DSPE-PEG(2000) (4%), and POPC:DSPE-PEG(2000) (4%) through the temperature range studied. Lines connecting the data are presented simply to aid the eye.

The permeability rate constants for DPPC:MPPC(10%) in Fig. 4 indicate minimal gel phase permeability below 37 °C, virtually identical to DPPC over the same temperatures. For this LTSL, however, permeability rate constants begin to increase at ~38–39 °C and reach a peak (0.372/min) at the membrane phase transition temperature, ~40.5 °C (each temperature is a separate sample). At the slightly higher temperature of 41 °C (also separate sample), the rate constants drop below this peak and then continue to increase slightly as temperatures higher than this are measured (using subsequent separate samples). It should also be noted that the liquid phase permeability rate constants for the LTSL are substantially higher than those of liquid phase DPPC or liquid phase POPC (see Discussion).

Rate constants for DPPC:MSPC(10%) formulation shown in Fig. 4 also indicate minimal gel phase permeability through 39 °C, virtually identical to DPPC. At higher temperatures (again, each temperature is a separate sample), substantial rate enhancement is noted, reaching a peak at 41.3 °C (T_m), the rate constants being just slightly lower than at the T_m peak for the DPPC:MPPC composition. At higher temperatures above T_m, the rate constants through the liquid phase membrane drop below this maximum, but remain above the pure DPPC and POPC, and just slightly lower than the MPPC formulation. Note though, that all the liquid phase permeability rate constants appear to be approaching common values at temperatures in the range of 50 °C and above.

To start to explore the permeability mechanism and how it relates to melting of the solid lipid bilayer microstructure, a plot of ion permeability rate constants for DPPC:MPPC(10%)

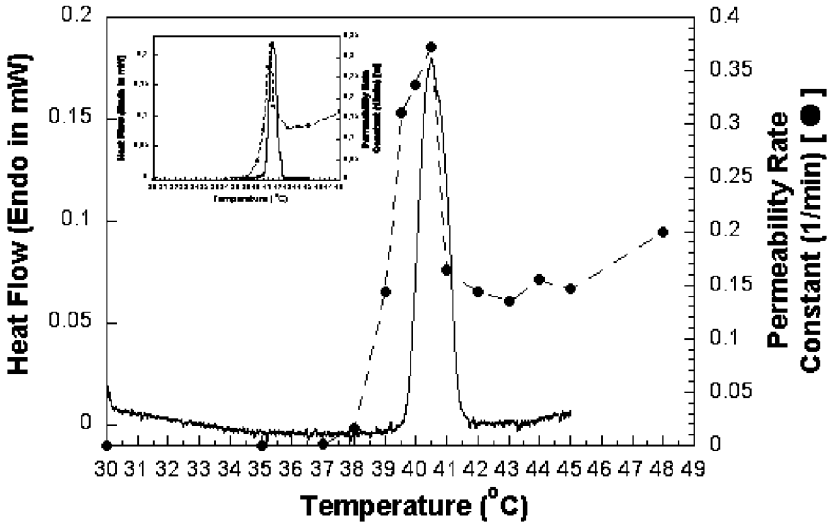

Fig. 5. Calorimetric data and permeability rate constants. Calorimetric data (endothermic heat flow in mWatts—solid line) and dithionite ion permeability rate constants (1/min—solid circles and dashed line) for DPPC:MPPC(10%):DSPE-PEG(2000) (4%) membranes and DPPC:MSPC(10%):DSPE-PEG(2000) (4%) membranes (inset) are shown as a function of temperature.

plotted together with DSC heat flow data is shown in Fig. 5. Note that the permeability begins to increase dramatically just above 38 °C and is already almost a maximum at 39 °C, yet the heat flow only starts to become significant (proportional to mass of lipid melted) near 39.5–40 °C. The permeability rate constant peak coincides with the thermal T_m at 40.5 °C. A similar plot for the DPPC:MSPC(10%) composition is shown in the inset of Fig. 5. Liposome membrane permeability starts to increase at just above 39 °C, with significant melting starting at ~40.5 °C. Again, it is important to note that the peak in permeability rate constant coincides with the transition midpoint at 41.3 °C.

The results from the experiments designed to determine whether the enhancement mechanism was related to lysolipid desorbing from the membranes or the presence of defect-stabilizing lysolipid remaining in the membranes are presented in the following figures. In Fig. 6, dithionite ion permeability rate constants are shown for pure DPPC, the DPPC:MPPC(10%) formulation as made, and a separate DPPC:MPPC(10%) formulation after being dialyzed for 48 h at 45–48 °C. It is important to note from this figure that following the elevated temperature dialysis, ion permeability rate constants are nearly identical to the non-dialyzed samples in both the gel (30–38 °C) and liquid phase regions (42–48 °C). In addition, the initial drop in relative absorbance during the dithionite permeability experiment (outer monolayer reaction) was still to ~0.42 of the original unquenched value. These results indicate the presence of stable bilayer vesicles below and above the transition temperature. Importantly, they also suggest that lysolipid is still present in the membranes since the temperature of the peak values is the same and the ion permeability rate constants are a little lower but still similar to undialyzed samples, and the enhancement in the liquid phase is still noted. If the lysolipid had desorbed, the permeability should have dropped back down to the level of DPPC over the whole temperature range. Although the rate constant near T_m at 40 °C appears to be slightly slower than for the undialyzed sample, (~1.4 times slower), the relative absorbance data are actually quite comparable, and subtle differences are simply enhanced with the exponential curve fit.

The results of the experiments of adding MPPC (equivalent to 3 mM in solution) to the outside of preformed DPPC indicated that the permeability rate constants throughout the temperature range are nearly identical to the results from the formulation with lysolipid present during the liposome formation process and equilibrated with 1 micromolar lysolipid during this processing (data not shown). This indicates that lysolipid can exchange into the membrane and provide defect permeability in the transition region and liquid phase mem-

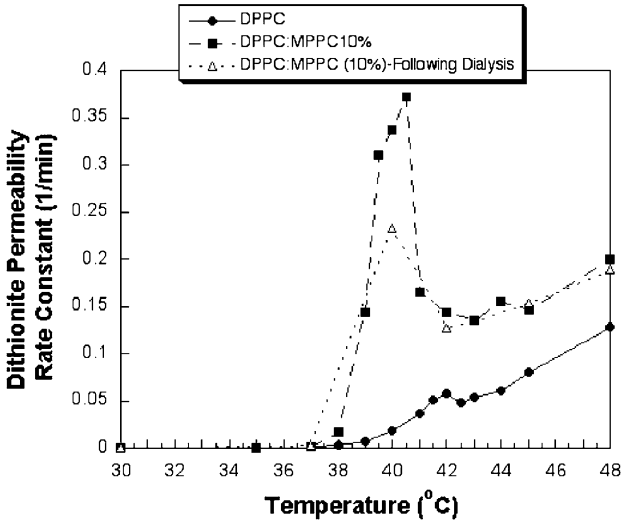

Fig. 6. Ion permeability rate constants following dialysis. Plot of dithionite ion permeability rate constants (1/min) versus temperature for DPPC:DSPE-PEG(2000) (4%), DPPC:MPPC(10%):DSPE-PEG(2000) (4%) and DPPC:MPPC(10%):DSPE-PEG(2000) (4%) following 48 h of dialysis at 45–48 °C.

branes. These results also support the conclusion that the presence of lysolipid in the membrane is necessary for the permeability enhancement. Experiments were also performed with lysolipid both in the membranes, and added to the external volume (as 0.3 mM micelles). Virtually identical rates were measured at all temperatures, further supporting the conclusion that the presence, rather than the desorption (or absorption) of lysolipid from the membrane is required for the permeability enhancement in a sample that already contains lysolipid in the gel phase membranes, and then is simply heated to the transition where enhanced permeability occurs.

Results from the Thin Layer Chromatography and Nuclear Magnetic Resonance analyses of the dialyzed samples of DPPC:MPPC(10%):DSPE-PEG(4%) also suggested that lysolipid was not desorbing out of the membrane into the external dialysate, even after the second change of dialysate and orders of magnitude dilution into what would be nanomolar concentrations (data not shown). TLC analysis of the solution remaining inside the dialysis bag revealed three clearly visible spots corresponding to DPPC, DSPE-PEG and MPPC. Only two spots were noted in the DPPC:DSPE-PEG(4%) sample, demonstrating that the MPPC signal was not simply due to hydrolysis of DPPC to MPPC during the dialysis procedure, and that it was retained in the liposome sample. The TLC and iodine spot method can detect lipid amounts on the order of 0.1 μg [46]. The amount of MPPC in the dialyzed samples (assuming no desorption) would be on the order of 7 μg, well above the limit of detection. The results from the NMR analysis of the dialysate solution (i.e., solution outside the dialysis bag) did not reveal any prominent peaks below 3.4 ppm that would correspond to protons associated with lipid. The limit of detection of proton NMR is on the order of a few tenths of a milligram of compound [47]. If all of the lysolipid had desorbed, it would be well within this limit (~1 mg), but certainly, this method cannot detect smaller fractions of lysolipid that may have desorbed. While it appears that large amounts of MPPC are not desorbing from the lipid membranes into the dialysate, even at temperatures above T_m, an absolute and calibrated quantitative measurement is not available at this time.

3.2. Activation energy determination

The temperature dependence of the ion permeability rate constants can be expressed in terms of the Arrhenius equation as:

$$\text{Permeability Rate Constant} = A^{*}\exp(-E_a/\text{RT}) \quad (5)$$

Where A is a pre-exponential constant and E_a is the energy of activation for the permeation. This relationship assumes that both A and E_a are independent of temperature. The activation energy for the ion permeability can be calculated by taking the natural log of Eq. (5):

$$\ln(\text{Permeability Rate constant}) = \ln A - E_a/\text{RT} \quad (6)$$

A plot then of the natural log of the Permeability rate constants vs. $1/T$ (absolute temperature in K) is linear with an intercept $\ln A$ and slope $-E_a/R$, as long as the activation energy is independent of temperature (i.e., data in the transition region are shown by not included in any slopes). Permeability rate constants for all of the membranes studied are plotted in Fig. 7 vs. $(1/T)\times 1000$ (K^{-1}). (The data points at 52 °C were not used when making the Arrhenius plots as not all compositions were measured at this temperature.) The solid lines drawn on the plot represent the slopes used to calculate the activation energies for POPC and DPPC (the other membranes were analyzed in the same manner). As expected, since it does not have a transition in the temperature range studied, only the POPC data showed a linear relationship over the entire range, since it was liquid at all temperatures. From the slope of the POPC data, the E_a for dithionite permeability through this liquid state membrane was calculated to be 36.4 kCal/mol. The other membrane compositions all showed a peak at their transition temperatures, indicating a temperature dependence in the activation energy at the phase transition as expected, and so this transition data was eliminated from any Arrhenius analysis.

For DPPC and both LTSLs, linear fits were made of the low temperature regions (~3.3–3.22 (1000/K), ~30–38 °C) and high temperature regions (3.17–3.11 (1000/K), ~43–48 °C) to calculate the activation energies through the gel and liquid state regions respectively. The activation energies for all membranes, along with literature values for the activation energy for water, and several ions and non-electrolytes are shown in Table 1. It should be noted that the liquid state regions of the DPPC, DPPC:MPPC(10%) and DPPC:MSPC(10%) membranes are not pure "liquid" phase regions as the membranes most likely still contain interfacial regions that have not completely melted.

3.3. Doxorubicin release

A recent paper by Ickenstein et al. shows that repeated cycling through the main acyl melting transition temperature

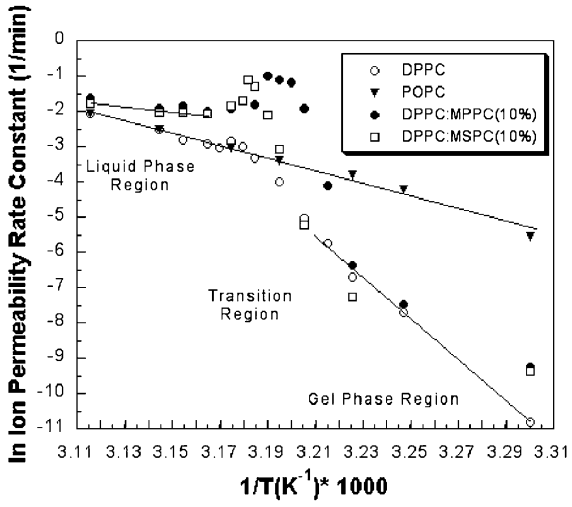

Fig. 7. Arrhenius plot of dithionite ion permeability rate constants through DPPC:DSPE-PEG(2000) (4%), POPC:DSPE-PEG(2000) (4%), DPPC:MPPC (10%:DSPE-PEG(2000) (4%), and DPPC:MSPC(10%):DSPE-PEG(2000) (4%) vesicles. The ln of the permeability rate constants are plotted against 1/Temperature (degrees Kelvin) × 1000. Solid lines on the plot illustrate the portions of the graph that were linearly fit to calculate the activation energy.

Table 1
Activation Energies for the gel and liquid phase regions computed from dithionite ion permeability measurements

Liposome composition	Activation energy (kCal/mol)	
	Gel phase region	Liquid phase region
POPC:PEG(4%)	N/A	36.4
DPPC:PEG(4%)	127.9	36.34
DPPC:MPPC(10%):PEG(4%)	103.7	11.74
DPPC:MSPC(10%):PEG(4%)	102.9	11.37

Solute	Activation energy (kCal/mol) through liquid membrane
H^+	18.4 [53]
K^+	15.1 [53]
Cl^-	17.9 [53]
Na^+	23 [1]
O_2^-	11.5 [54]
Glucose	25.7 [53]
Fructose	21.5 [53]
Glycerol	11 [55]
H_20	9.8 [52]
Urea	9.3 [55]

Lower table shows activation energies from the literature for various solutes through liquid phase vesicles.

converts a lysolipid-containing liposome sample to one of stabilized disc particles (disk-like micelles) [12]. Interestingly then, this cycling appears to disrupt the soccer-ball morphology of the micrograins structure of these 100 nm scale liposomes—grain structures that we have previously seen in DMPC Giant Unilamellar Vesicles using micropipette manipulation (Needham and Evans, unpublished results), DSPC monolayers on gas bubbles [10] and in the drug containing liposome samples themselves by TEM [12]. In order to check for disk formation, and rule out this potential drug releasing mechanism for our single-cycle heating protocol, the particle size results from a Photon Correlation Spectroscopy analysis of an extruded DPPC:MPPC(10%):DSPE-PEG(4%) Doxorubicin-loaded sample indicated a mean diameter of 120.7±27.7 nm. To determine whether the LTSL changed size or converted to disc-like micelles following a single heating through the transition temperature, size measurements at a scattering angle of 90° were made on the same sample after heating to 40.5 °C and maintaining this temperature for 30 min. The mean size before and after heating remained virtually identical at ~120–122 nm, indicating that disc formation did not occur under the conditions of our one scan heating test, as would be experienced in use in clinical applications. Permeability results then were solely due to membrane transport and not vesicle disruption into membrane disc fragments. Although an interesting observation in and of itself, since it shows how lysolipid can possibly stabilize gel phase bilayer edges when micrograin boundaries create the disc templates, and points to lysolipid pores at such boundaries as a possible precursor to full micellization, it appears that disc formation due to stabilization of membrane fragments requires many multiple cycles of heating and cooling through the transition region.

To further support the conclusion that the LTSL vesicles remain as intact bilayer membranes even after heating to T_m, direct microscopic observations were made of large (20–30 μm) vesicles, before, during and after heating through the main phase transition using the micropipette manipulation methods described above. This temperature cycling was repeated four times on the same vesicle demonstrating that the vesicles remain intact throughout the phase transition, even though the membranes contain lysolipid. These in situ observations of a vesicle cycling through the phase transition again indicate that the mechanism of drug release is not due to break up or disc-micellization of the bilayer membrane.

A representative set of data from the doxorubicin release measurements is shown in Fig. 8 as moles of DOX released

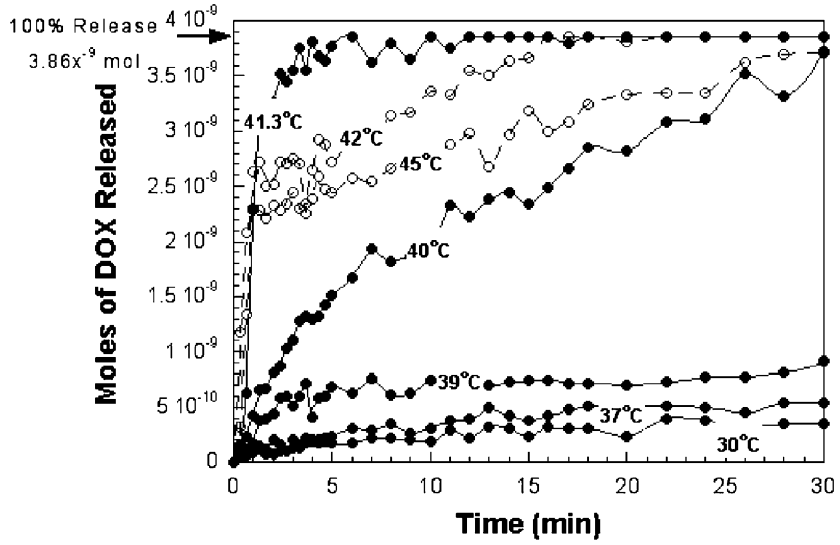

Fig. 8. Moles of Doxorubicin released versus time in minutes from DPPC:MSPC(10%):DSPE-PEG(2000) (4%) vesicles at 30, 37, 39, 40, 41.3, 42 and 45 °C. The release of 3.86 e^{-9} moles of drug corresponds to 100% release of contents. All data points represent the mean of three separate experiments. Open circles represent release at temperatures above the transition temperature.

versus time in minutes from the DPPC:MSPC(10%) formulation demonstrates that, as a result of its slightly higher T_m, the formulation is fairly stable up to 39 °C, releasing only 10–15% over the course of 30 min at these temperatures. Drug release rapidly increases when the liposomes are heated to ~40 °C, with 80–100% of encapsulated contents released within 20–40 s at 41.3 °C (T_m). At 42 and 45 °C, biphasic release curves are noted, where initial release is very rapid as the liposomes pass through the transition region, but then slows when the vesicles completely melt and reach the desired measurement temperature above 41.3 °C.

To calculate release rates at each temperature for each composition, the method represented in Fig. 9 was used. Moles of DOX released (open circles) are plotted on the left hand *Y*-axis versus Time in seconds on the *X*-axis. Plotted on the right hand *Y*-axis is the temperature of the sample (corresponds to solid line) demonstrating the rate of heating as the samples were transferred from room temperature into the circulating water bath, equilibrated to 40 °C for this trial. Once the sample temperature reached 40 °C (~40–60 s), a curve fit was used to determine the initial rate of release of the linear portion of the data as demonstrated by the short-dash line. The slope of this line, $m1$, is the rate of DOX released in Moles/second when the sample reached the measuring temperature of 40 °C. A linear fit was used as this was found to best represent the initial rate of rapid release that was noted in formulations at or near the phase transition.

Fig. 10 shows the calculated DOX release rates (moles/second) versus temperature for DPPC:DSPE-PEG(2000) (4%) liposomes, and the DPPC:MPPC(10%):DSPE-PEG(2000) (4%) and DPPC:MSPC(10%):DSPE-PEG(2000) (4%) temperature-sensitive formulations. For DPPC, a slight peak in the DOX release rate is noted at T_m (42 °C) which is ~5 times greater than the release rate at 37 °C, demonstrating, however,

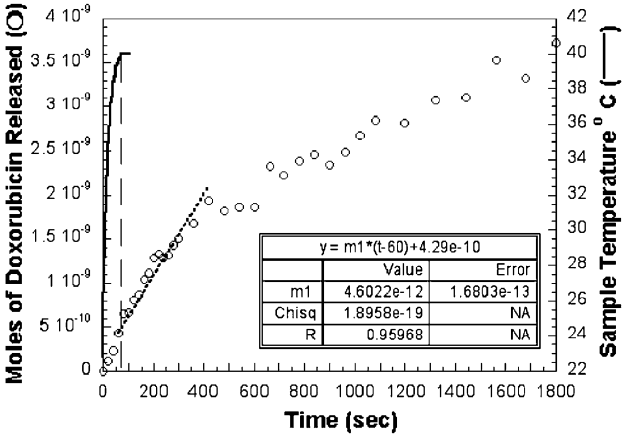

Fig. 9. Method used to obtain Doxorubicin release rates in moles/second. Moles of Doxorubicin released from DPPC:MPPC(10%):PEG(4%) vesicles are plotted (open circles) versus time in seconds. Along the right hand *Y*-axis, the sample of the temperature is plotted as it is raised from room temperature to 40 °C (corresponds to solid line). The long dash, vertical line indicates the time at which the sample reaches 40 °C, approximately 40–60 s. The initial linear portion of the release curve was then fit (i.e., once the sample reached the measuring temperature of 40 °C), with a straight line as indicated (short dash line). The constant, $m1$, is the release rate in moles/second.

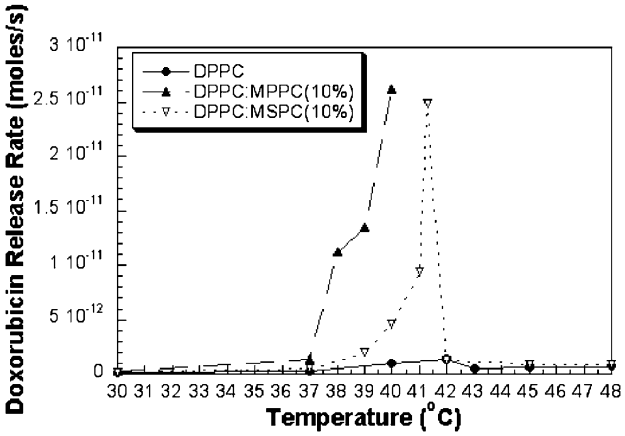

Fig. 10. Doxorubicin release rates (Moles/second) for DPPC:DSPE-PEG(2000) (4%), DPPC:MPPC(10%):DSPE-PEG(2000) (4%) and DPPC:MSPC(10%):DSPE-PEG(2000) (4%), versus temperature. Lines connecting the data are presented simply to aid the eye.

only a modest rate enhancement at the transition temperature above the relatively impermeable solid phase. Release rates for the DPPC:MPPC formulation begin to increase substantially near 38 °C, reaching an apparent maximum at 40 °C that is ~650 times greater than its relatively impermeable gel phase and nearly 25 times above pure DPPC at the same temperature. Rates above 40 °C could not be determined as 100% release of all contents occurred rapidly, before the liquid phase temperatures were ever reached. Release rates from the DPPC:MSPC formulation were similar to DPPC through ~37 °C and then rose considerably near ~39 °C. At the phase transition, the release rate was 55 times greater than through its gel phase membranes at the clinically relevant 37 °C, and ~20 times greater than pure DPPC at the same temperature (41.3 °C). At temperatures greater than T_m, the rates dropped back down in the liquid phase region, just slightly higher than for the pure DPPC liquid phase.

4. Discussion

The addition of single chain lysolipids to pure DPPC bilayers has produced a dramatic enhancement in the main phase transition permeability of the membranes for permeability markers such as carboxyfluorescein and dithionite, and for the chemotherapeutic drug Doxorubicin as shown here. Based on the data presented above, it appears that this enhancement is due to permeation through transmembrane lysolipid-stabilized porous structures initiated at the grain boundaries in a melting membrane in the gel to liquid crystalline phase transition region. This effect enhances the already recognized packing mismatches that seem responsible for the anomalous permeability for pure lipid melting transitions [2]. Together, with discussion of the data, the following discussion will present several arguments that support this conclusion.

4.1. Enhancement of dithionite permeability

Taking non-lysolipid containing membranes first, a comparison of the ion permeability rate constants in Fig. 4 of the

gel phase region of DPPC (30–38 °C) with liquid phase POPC at the same temperatures show that the DPPC permeability rate constants to the ionic species of dithionite are ~20-fold below those of the liquid phase POPC, and have an activation energy difference of a factor of about 4 (Table 1). This difference demonstrates the relative impermeability to ions of the condensed, solid phase lipid compared to a liquid phase membrane at the same temperature. As melting initiates at pre-existing DPPC grain boundaries (>39 °C), the permeability rate constants increase as liquid regions form, resulting in leaky interfaces between solid domains and melting liquid regions [2]. At the transition temperature (42 °C), the area of these highly disordered interfacial regions attains a maximum value, accounting for the ion permeability rate constant enhancement above that for pure liquid phase POPC at the same temperature. While the ion permeability rate constant at the transition temperature is nearly 130 times faster than through gel phase DPPC (35 °C), it is important to note that this enhancement is relatively small, only ~1.5 times above liquid POPC at the same temperature. In the liquid phase (DPPC > 42.5 °C), both membranes exhibit virtually the same inherent permeability to the ion, eventually (at temperatures only 2–3 degrees C above T_m) reaching rates higher than those measured during the phase transition anomaly at T_m.

Examining the transition itself, a correlation can be made between permeability and membrane compressibility. In transition regions for a range of lipid compositions, membrane permeability and, especially, water permeability have previously been shown to directly correlate to membrane compressibility, expressed as compliance [48]. Evans and Kwok have also shown that the area expansion modulus of membranes does in fact decrease in the transition region for a giant lipid vesicle. For example, the modulus of dimyristoylphosphatidylcholine (DMPC) liquid phase (a diC14 chain lipid, T_m=24 °C) is ~125 mN/m [5], while DMPC solid phase is ~850 mN/m [34], nearly 7 times as cohesive. But, at the phase transition temperature, the vesicle membranes have an area expansion modulus of only ~20–30 mN/m [5], demonstrating the highly compressible nature of the bilayer in this region. Theoretically the area expansion modulus goes to zero at a first order transition, i.e., the membrane becomes infinitely compressible. But in reality, the lipid transition is pseudo first order [2], and the elastic modulus approaches low (but non-zero) values, possibly due to even slight impurities in the bilayers [5]. And, since in general, for all membrane compositions measured to date, the more compressible the membrane, the more permeable the bilayer is to water and other small molecules, we might expect, from mechanical (continuum) arguments, that the permeability characteristics through the transition region would also be directly related to the elastic area expansion modulus (K_a) of the membranes and so increase dramatically at the transition, which it does. For DPPC, permeability through the dense, solid phase was, as expected, substantially lower than through the more compressible, liquid phase. The surprising result, in the light of recent modeling [2,8] and earlier experiments [1], was that the ion permeability, at the extremely compressible phase transition region, was only 1.5 times greater than through a similar liquid phase lipid at the same temperature (and appears to involve the melting and chain mismatch at these melting boundaries for DPPC, that are obviously absent from a purely liquid bilayer like POPC at 42 °C [49]).

In contrast, measurements of the lysolipid temperature-sensitive liposomes demonstrate a dramatic permeability enhancement at the phase transition due to the presence of lysolipid in their bilayer prior to heating through T_m. Permeability rates through the DPPC:MPPC(10%) gel phase vesicle membranes (<37 °C), are nearly identical to the pure gel phase DPPC vesicles, and are stable up to body temperature (37 °C). One of the most important pieces of data from this study is shown in Fig. 5 where a significant increase in permeability starts at the shoulder of the DSC trace (~39 °C), before any significant melting of the LTSL membranes, implying a role for melted grain boundaries. DPPC:MPPC permeability rates at 39 °C are nearly 20-fold above gel phase DPPC and approximately 5 times higher than the liquid phase POPC at the same temperature. The postulated lysolipid-stabilized pores enhance the ion permeability through the membrane far above not only what was measured through a gel phase/melting DPPC bilayer, but also through a pure liquid POPC vesicle. The rate enhancement reaches a peak at the transition temperature of the LTSL (~40.5 °C), that is nearly 20-fold higher than DPPC at the same temperature, and ~650-fold higher compared to permeability through the gel state (35 °C). After the bilayers melt (>40.5 °C), the permeability drops below the peak maximum as the interfacial area (between remaining solid and melted domains) starts to reduce, but remains ~2–3× higher than liquid state DPPC or POPC membranes, indicating the continued role of possible lysolipid stabilized defects in persistent microstructure (see later in Discussion).

The DPPC:MSPC(10%) formulation also exhibits low ion permeability rates in the gel phase, similar to pure DPPC. The addition of the longer chain C18 lysolipid not only raises the transition temperature relative to the DPPC:MPPC formulation by 0.7 °C, but also slightly increases the temperature at which significant ion permeability initiates from ~38 °C to 39 °C, which may be important in the clinical use of the formulation where the liposome has to be stable and not release drug at 37 °C, but can be triggered to release above body temperature, but not too high that it can't be reached by mild hyperthermia. As with pure DPPC and the MPPC formulation, the peak in permeability coincides with the peak in the transition as shown in Fig. 5. The ion permeability rates through the MSPC containing membranes at the transition temperature are more than 600 times faster than through the gel phase membranes, and nearly 10 times as fast as DPPC at the same temperature (41.3 °C).

To reiterate now for all membrane systems, the most telling characteristic regarding mechanism of permeability, is that permeability begins to increase significantly prior to any significant melting of lipid registering on a calorimetric scan (Fig. 5). In all cases, the enhancement initiates before any significant shoulder of the DSC trace. Examining the rates as a

function of relative temperature, T/T_m, provides a comparison of the point at which permeability begins to increase for each membrane (plot not shown). Enhanced permeability through all membranes begins at nearly the same relative temperature (~0.992), with the DPPC:MPPC formulation initiating at perhaps a slightly lower relative temperature than the other two membranes (~0.990).

Mouritsen's dynamic models of the phase transition region indicate that, in DPPC membranes, interfacial areas between the solid phase membrane and newly melted regions begin to form, starting at the intergrain boundaries just above 37–38 °C [2,13]. Based on this, his model of the relative permeability indicates that significant enhancement begins at a relative temperature near 0.99 for DPPC vesicles, and this is confirmed by our results. Mouritsen's models also suggest, surprisingly, significant interfacial regions exist far beyond T_m, out to near 47–48 °C for DPPC [13]. If this were true in real membranes, then, at these interfacial regions, for membranes that contain lysolipid, lysolipid stabilized pores could still exist, accounting for the moderate enhancement noted in the liquid phase LTSLs that still existed at values above those of liquid DPPC and POPC membranes. At higher temperatures (data at 52 °C in Fig. 4), it is expected that no interfacial regions remain, and the permeability rate constants through the liquid state DPPC and liquid state DPPC:MSPC(10%) are at virtually the same level. The slight enhancement still noted with the MSPC is most likely due to the presence of the single chain second component lipid, as supported by POPC:MPPC data presented later which also shows a slightly enhanced permeability. A more detailed description of the enhancement mechanism is provided below.

In the Arrhenius plots (Fig. 7), DPPC and both LTSLs showed a peak at their transition temperature, indicating the expected temperature dependence in the activation energy at the phase transition. This peak due to the presence of liquid–solid interface region contrasts the discontinuity noted in other two-phase systems [50,51].

In the Arrhenius plots (Fig. 7), the activation energy through POPC and liquid state region DPPC was determined to be ~36 kCal/mol. As expected, values for the three gel state membranes demonstrated a much greater barrier to the ion permeability. For DPPC membranes, E_a was ~128 kCal/mol, nearly 4 times that of the same membrane in its liquid state. For both of the lysolipid membranes, the energy barrier is similar but slightly lower than this pure lipid value at ~103 kCal/mol. While the energy barrier to permeability for both liquid phase DPPC and POPC was nearly identical at 36 kCal/mol, a significant drop is noted for both liquid phase LTSLs to ~11 kCal/mol, in line with them being much more permeable in the liquid phase region, where the lysolipid introduces a chain vacancy defect per molecule (as well as the presence of interfacial regions that still remain), in a temperature range just above T_m.

For comparison, E_a for water permeability through the liquid phase membranes of SOPC (C18:0–C18:1, T_m = ~6 °C) has been measured at room temperature to be approximately 9.8 kcal/mol [52] and E_a for Na^+ permeability through DOPG membranes (T_m = −18 °C [23]) was determined to be ~23 kcal/mol [1]. The activation energy for dithionite ion permeability through a liquid phase membrane would be expected to be a fair amount higher than the activation energy associated with water permeability due to the negative charge of the ion, and be slightly greater than the energy required to transport the smaller sodium ion, radius ~1.9 Å vs. 3 Å for SO_2^-, through a liquid membrane. The results for liquid phase DPPC and POPC then seem to be reasonable.

The activation energies for the liquid phase region LTSLs are quite low, at or below those measured for water and several non-electrolytes that transport presumably through homogeneous lipid membranes (see Table 1) [53–55], and so represent additional evidence that ion transport is through a more aqueous pore than through the lipid per se in this transition region. Above T_m, as noted above, interfacial regions are hypothesized to persist at temperatures up to ~48 °C in the LTSL membranes. The energy barrier here may be associated with both permeation through the pure liquid state of the bilayer, containing the 10 mol% chain vacancy defects, and a characteristic of lysolipid pores still present at the few but remaining interfacial regions that facilitate ion transport, providing some experimental evidence for their existence above the transition region as postulated by Mouritsen et al. [2].

4.2. Enhancement of doxorubicin release

Concerns about constant excitation bleaching the fluorescent signal from DOX dictated that the drug release experiments were performed on individual samples as outlined in Materials and methods. As a consequence, for release experiments conducted at temperatures above T_m, every sample was heated (quickly) through the transition on its way to the desired liquid state temperature. Only after the sample reached the desired temperature could accurate rates be calculated (as demonstrated in Fig. 9) since the initial jump in release was due to permeability through the transition region.

For the DPPC:MPPC formulation, accurate permeability rates could only be calculated up to the transition region, near 40 °C. Measurements for liquid state vesicles could not be made, since by the time the membranes reached the temperature of interest (taking ~40–60 s), 100% of the drug had already been released as they passed through T_m. (This release is certainly a desired effect for performance in any clinical application for drug delivery to the tumor, but compromises to some extent these studies concerning characterization of drug release in vitro.) In the case of the DPPC:MSPC formulation (Fig. 8), a biphasic release curve is noted for temperatures above T_m. The initial 20–40 s of release for 41.3 °C and 42–48 °C was nearly identical as the membranes passed through the transition region. As they were heated above the region (again taking 40–60 s), a measurement of the release rate through the liquid state membrane could then be made, with the remaining doxorubicin leaking out, showing that release rates did slow down above T_m.

The data in Fig. 10 demonstrate a dramatic 20-fold enhancement in the Doxorubicin release rates of the DPPC:

MSPC LTSLs above pure DPPC liposomes at the transition. As loaded, the DOX in the liposomes is complexed and crystallized at low pH and is not permeable through the membrane. Only a tiny fraction of drug (less than 0.01%) is expected to be non-protonated at this pH of 4. It is unlikely then that drug is leaking out of the vesicles in this region via a simple lipid membrane solubility mechanism (even though the lipid melts, the membrane is still intact and represents largely, over most of its area, a hydrophobic low dielectric constant barrier to ion flow). In their transition region though, the presence of grain boundaries and the possibility of lysolipid pores and the rapid release of drug suggest that the entire contents of the liposome, both the hydrophobic unprotonated DOX and the larger fraction of membrane non-permeable $DOXH^+$, as well as the citrate buffer and dissipation of the pH gradient, are crossing the bilayer. As noted in the dithionite permeability data, drug permeability enhancement starts almost 2 °C before the midpoint of the main calorimetric transition, adding additional support to the permeability enhancement of leaky membrane interfacial regions near 38 °C. Measurements of the liquid phase DPPC:MSPC vesicles indicate that the release rates drop back to levels just slightly above those for the DPPC bilayers. Since approximately 50% of the encapsulated drug leaked out of the vesicles as they were heated through the transition, the pH gradient across the bilayer most likely diminished as well. Therefore, the measured values may not necessarily reflect the true release rates for a liquid state membrane if it could be made to start at this temperature with the same internal amount of drug and concentration gradient starting condition. Ideally, the release rates above the transition could be measured on a single sample, heated much more rapidly so as to limit release of drug and H^+ ions in the transition region, but we did not achieve this in the present study.

Although experimental factors limited the ability to measure the true Doxorubicin release rates above the transition temperature, the results presented here provide important and clinically relevant data. In clinical treatment scenarios, liposomes could be introduced intravenously to the patient after heating the tumor to the desired temperature of a mild hyperthermia treatment, around 40–42 °C. The liposomes would be elevated from body temperature (37 °C) to the hyperthermic temperature in the heated tumor region, even in the blood stream of the tumor, at a rate comparable to the experiments performed here. Based upon these experiments, if liposomes, as they flow through the tumor vasculature, are exposed to temperatures in the range of ~40–42 °C for as little as 40–60 s, significant amounts of drug (80–100%) would be released from each liposome passing through the heated region. Of course, sustained and continued heating would allow greater numbers of liposomes to pass through and release their contents in the blood stream. Since transit times through tumors are on the order of only a few microns per second, release time matches or is less than transit time of the blood borne liposomes through the tumor and so drug release is immediate, and if in the blood stream, would also possibly affect the endothelial cells as well. This represents a new paradigm for local drug delivery. Rather than designing for, and relying on serendipitous liposome extravasation into tumor tissue, the application of mild hyperthermia producing triggered drug release in the blood stream, allows for diffusion into both endothelia and tumor tissue and adds an additional advantage in therapy. Of importance to clinical application is our in vitro result that, if the final temperature obtained is much above 42 °C, and if the rate of heating of the liposomes as they pass into the heated tumor region is such that the membranes do not spend sufficient time in their transition region, the rate of release could diminish significantly at these (even slightly) higher temperatures and a much smaller amount of drug would be supplied to the tumor than if the temperature was maintained at just below or at the phase transition midpoint temperature of 41.3 °C. The composition and material state of this liposome membrane undergoes a very sharp and critical transition and drug release mechanism, and has been designed to be so. It is probably unlikely that the heating rates in vivo (normally about 1 °C/min—personal communication R. McGough, Department of Radiation Oncology, Duke University Medical Center) would approach those used in these experiments (~15 °C/min), so this may not be a concern, and all drug is expected to be released from the liposomes as they attain hyperthermic temperatures in the 40–42 °C range, even in the blood stream, possibly, as mentioned, obviating a necessity to allow time for and require extravasation into tumor tissue [11]. With respect to action on endothelial cells of the tumor blood vessels, what we have seen is that before treatment, the red blood cell (RBC) velocity in tumors was 0.428 ± 0.037 mm/s and the microvascular density was 3.93 ± 0.44 mm/mm^2. At 24 h after the treatment, they were reduced to 0.003 ± 0.003 mm/s and 0.86 ± 0.27 mm/mm^2, respectively. The same treatment, however, caused only a 32% decrease in the RBC velocity and no apparent change in microvascular networks in normal subcutaneous tissues over the same period. And so, the rapid release of DOX during hyperthermia allows the drug to shutdown tumor blood flow while having only minor effects on normal microcirculation in subcutaneous tissues [66]. In some tumors, few functioning blood vessels are left remaining in the tumor, and the blood flow is essentially zero. The formulation and rapid mode of delivery and location of drug release then look to be able to provide an anti-vascular as well as anti-cancer cell mechanism of anti-tumor therapy.

The permeability data presented here clearly demonstrate the dramatic enhancement in both ion permeability and drug release rates that the incorporation of lysolipid creates above single component lipid membrane systems. It is interesting then to make a comparison between the release rates for the two molecules by examining the permeability coefficients at the transition temperatures of the pure DPPC and the DPPC:MSPC(10%) liposome systems (the permeability coefficients for DPPC:MPPC(10%) were not calculated since DOX data was not available at the transition temperature).

The data from the dithionite permeability measurements were curve fit using Eq. (4) above, which can be represented as:

$$C(t) = C_0 \exp(-m2^*t) \tag{7}$$

where $m2$ is the permeability rate constant, $C(t)$ is the concentration of un-reacted NBD molecules at time t, and C_o is the concentration of un-reacted NBD molecules on the inner monolayer at time zero (i.e., when the dithionite was added). For dithionite ion permeability, the number of dithionite ions added to the cuvette outnumbered the NDB molecules by 1000:1, and it was assumed that once an NBD molecule reacts, it does not dissociate from the bound state (supported by experiments measuring NBD-lipid flip-flop that last hours to days [56]). The measured rate, $m2$ from Eq. (7), can be expressed in terms of the permeability coefficient [65] as

$$m2 = S_1 P / V_1 \tag{8}$$

Solving for the permeability coefficient, P and reducing the equation yields

$$P = m2^* V_1 / S_1 = m2^* R/3 \tag{9}$$

Where R is the radius of the liposomes, ~60 nm. Based on this assumption, the Dithionite ion permeability coefficient for pure DPPC:DSPE-PEG(4%) at 42 °C and DPPC:MSPC(10%): DSPE-PEG(4%) at 41.3 °C can be calculated.

$$P_{SO2-} \text{ for DPPC} : \text{DSPE} - \text{PEG}(4\%) = 1.9^*10^{-9}\text{cm/s}$$

$$P_{SO2-} \text{ for DPPC} : \text{MSPC}(10\%) : \text{DSPE} - \text{PEG}(4\ \%) = 1.09^*10^{-8}\text{cm/s}$$

—a factor of five, then, for SO_2^-.

The release of doxorubicin from the membranes can be expressed as

$$dC/dt = -S_1 P / V_1 ^* C \tag{10}$$

where dC/dt is the change in concentration of the doxorubicin, S_1 is the surface area of the liposomes, P is the permeability coefficient, V_1 is the volume of the liposomes, and C is the initial concentration of the doxorubicin inside the liposomes.

From the Doxorubicin release measurements, the permeability coefficients can be calculated using Eq. (10), where the measured initial release rate in moles/second is dC/dt, the total encapsulating volume of the liposomes (V_1) in the test tubes was 61.8 nL, the total surface area of the vesicles through which the drug was permeating (S_1) was 119 cm^2, and the initial amount of drug inside of the vesicles (C) was 3.86×10^{-9} mol. The permeability coefficients for DOX are then

$$P_{DOX} \text{ for DPPC} : \text{DSPE} - \text{PEG}(4\%) = 3.4^*10^{-10}\text{cm/s}$$

$$P_{DOX} \text{ for DPPC} : \text{MSPC}(10\%) : \text{DSPE} - \text{PEG}(4\%) = 3.3^*10^{-9}\text{cm/s}$$

—a factor of ten for DOX.

Thus, the permeability coefficients at the transition temperature for both ion and drug are higher for the lysolipid containing membranes compared to the pure DPPC membranes, as expected from the release rates, by about an order of magnitude. Comparing the ion and DOX permeability, for the pure DPPC membranes, the permeability coefficient for the dithionite ion (radius ~3 Å) is about six times larger than the coefficient for the DOX molecule (radius ~500 Å), demonstrating that the smaller ion can permeate the bilayer more easily. For the DPPC:MSPC(10%) membranes, the permeability coefficient for dithionite is only about three times higher than the permeability coefficient for DOX through the same membrane. Since the permeability barrier is believed to be a water-filled pore (see below) rather than the hydrocarbon chain region, the larger size of the doxorubicin molecule plays less of a role in reducing the permeability coefficient through the lysolipid containing membrane than it does through the pure lipid membrane that presumably has less or no stabilized pores, relying more on solid/liquid acyl chain mismatches.

4.3. Proposed mechanism of permeability enhancement-lysolipid-stabilized pores

Detergents have been recognized since the late 1970s to cause membrane-spanning pores in liquid phase bilayers [57], and have been shown to increase phase transition permeability when subsequently added to pre-formed liquid-phase liposome suspensions [58]. Based on our dialysis experiments (where lysolipid, already in the liposome membranes, was found to remain in the membranes even upon extensive dialysis preserving the temperature-triggered permeability) and experiments where MPPC was incubated with preformed DPPC vesicles to produce the same results, it is our conclusion that lysolipid is an absolute requirement for the kind of high rates of solute permeation enhancement we have observed. It is though, the presence of lysolipid in both halves of the membrane, already present in solid solution prior to thermal processing, that distinguishes the LTSL mechanism for in vivo application from other thermal-sensitive liposome compositions and their performance. From TLC and NMR analysis, it also appears that very little, if any, lysolipid leaves the membranes in the liquid phase by wash-out, indicating that the enhancement mechanism does not seem to be due to desorbing lysolipid "leaving vacancy defects," as we might have originally thought. Based on the data presented in this paper, it now appears that the presence of lysolipid enhances the permeability of DPPC vesicles at the phase transition, presumably by stabilizing pores at melting grain boundary regions, even though equilibrating lysolipid is not present in the bathing medium. With this circumstantial evidence in hand, we now postulate mechanisms of permeability for each of the three regions, gel phase, transition and liquid phase regions.

4.3.1. In the gel phase

For the gel phase bilayers, ion permeability rates through both LTSL membranes were extremely low and virtually identical to those through the solid DPPC membranes. A slight difference in the activation energies between the two (~128 kCal/mol for DPPC vs. ~103 kCal/mol for LTSLs) may be a result of lysolipid being uniformly distributed throughout the solid bilayers. The mechanism of ion permeability through synthetic lipid bilayer membranes is still not fully understood. Several reports support the conclusion that ion permeability

through the bilayer occurs by a solubility–diffusion mechanism [49,59], where the ion must first partition in the membrane, then diffuse across the bilayer midplane, and finally partition into the internal aqueous phase [59]. This is the primary mechanism believed to account for water and non-electrolyte permeability [49]. Others believe that permeability occurs through short-lived, hydrated transient pores produced during thermal fluctuations [3,60]. Here, the permeating molecule avoids the energy barrier associated with the hydrophobic interior of the membrane.

In the gel phase region, solubility-diffusion into the lipid bilayer is most likely the dominant mechanism, since thermal fluctuations should be fairly small (in this highly condensed, high modulus membrane [34]). As hydrated ions approach the surface, they pass through the membrane by first partitioning, and then dissolving through the membrane. For gel phase lysolipid membranes, the single chain PCs pack normally at the interface (same head group) [61], but allow additional free volume in the hydrocarbon region due to their single chain per molecule and concomitant chain vacancy defect [18]. These packing or chain vacancy defects (at about 10 mol%) could facilitate transmembrane transport and lower the activation energy barrier for ion diffusion through the bilayer, especially at grain boundaries, even prior to melting, due to mismatches in packing at these crystalline structure-defects.

4.3.2. In the transition region

As the membranes begin to melt, liquid–solid interfacial regions form at existing grain boundaries. Although calorimetric changes (increase in endothermic heat flow) are not measurable until near 40–41 °C for DPPC (proportional to the mass of lipid melted), significant interfacial (solid/liquid) area is predicted to start to form near 38 °C, about 4 °C below the main transition temperature [13]. Similarly, fluorescence spectroscopy data from dimyristoylPC (DMPC, C14) vesicles indicate the formation of interfacial regions at ~20 °C, which is also 4 °C below the main transition for this lipid [62] as predicted by cooperative transition models [7]. These highly disordered interfacial areas account for the increase in permeability, and therefore an increase in their area directly corresponds to an increase in the ion permeability [2].

For the LTSL membranes, increases in the interfacial area start at slightly lower absolute temperatures, since T_m is ~1 °C lower than for the pure lipid DPPC membranes (the lysolipid slightly liquefies the membrane and the transition temperature is lowered by about a degree for inclusion of 10 mol% MPPC and 0.5 °C for inclusion of 10 mol% MSPC compared to the pure DPPC membrane). As soon as these grain boundary regions liquefy, lysolipid has the opportunity to form defect structures that stabilize pores along the highly compressible liquid–solid boundaries. As a result of their conical molecular shape (large head group, single chain) [63], and tendency to form spherical micelles in aqueous solution, these lysolipid molecules are well suited to form headgroup lined pores. Ions no longer have to interact with the low dielectric, hydrophobic region of the membrane, but can now pass through a headgroup lined, aqueous pore. Consequently, the permeability rates are dramatically higher than those of DPPC throughout the transition region, and about 6 times higher at the relative transition ($T/T_m=1$). The permeability rates through the MPPC formulation are ~1.1 times greater than through the MSPC formulation at $T/T_m=1$. Although both LTSL membranes should contain about the same amount of interfacial area, it appears that either the monopalmitoyl lysolipid forms more of the porous structures, or the pores that it forms are more stable, resulting in the slightly higher rate of ion permeability. This difference is not surprising since its shorter aliphatic chain (C16 for MPPC vs. C18 for MSPC) gives it a slightly more conical geometry, which should allow it to pack more easily into the hemispherical shape required in the pore [63] and match the hydrophobic thickness of the DPPC membrane.

4.3.3. In the liquid phase

Data for the LTSL membranes demonstrate an enhanced permeability above liquid DPPC from above T_m to ~48 °C. These results support two conclusions. (1) Lysolipid is still present in the membranes, and has not desorbed from the 100-nm vesicles. (2) Coupled with this, the continued enhancement is a result of the presence of solid/liquid interfacial regions and lysolipid-stabilized pores that persist up to ~48 °C. The models from Mouritsen suggest that interfacial regions exist out to 47–48 °C for DPPC liposomes, 5–6 °C above the mid point transition temperature [13]. Fluorescence spectroscopy data from DMPC vesicles also confirm the presence of grain interfaces 3–4 °C beyond the transition temperature in support of Mouritsen's model [62]. In addition, membrane thermal expansivity does not reduce to its steady state liquid phase value until a few degrees above the transition temperature of DMPC indicating the continued presence of some high compressibility, solid–liquid interfaces [34]. At temperatures above 48 °C, theory predicts that no interfacial areas remain, and the two membrane permeabilities (DPPC and DPPC:MSPC at 52 °C) coincide, with the minor enhancement from the presence of lysolipid over pure DPPC at 52 °C probably a result of increased free volume in the membrane, similarly noted for gel phase LTSLs.

Additional support for the presence of interfacial regions and lysolipid pores is presented in Fig. 11. Dithionite ion permeability rates are shown for DPPC, POPC, DPPC:MPPC(10%) and an additional system, POPC:MPPC(10%) where 10% MPPC was incorporated in this membrane during hydration, just as with the LTSLs. Lysolipid in the POPC liquid phase membranes causes only a very small increase in the permeability rates above pure POPC over the entire temperature range. Obviously, POPC membranes do not contain any grain structure and so this is as a result of a slightly increased free volume in the hydrocarbon region (one less chain per molecule on same PC headgroup introducing a chain vacancy). These measurements support the minor permeability enhancement noted at 52 °C for the DPPC:MSPC formulation. Importantly, the dithionite permeation rates through the POPC:MPPC vesicles are substantially lower than in the DPPC:MPPC liquid phase vesicles (42–48 °C). If the permeability enhancement in the liquid phase was only due

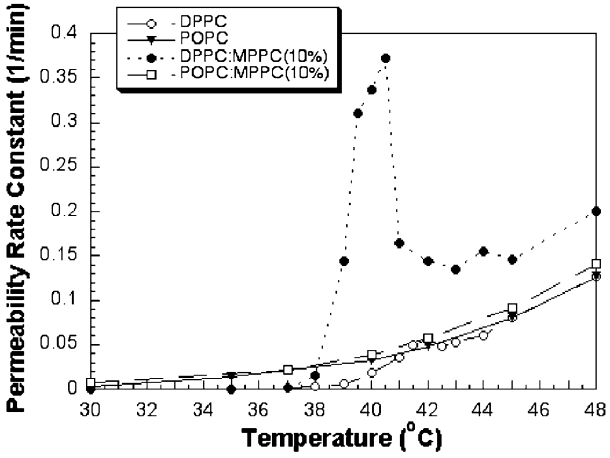

Fig. 11. Comparison of the dithionite ion permeability rate constants (1/min) through DPPC:DSPE-PEG(2000) (4%), POPC:DSPE-PEG(2000) (4%), DPPC:MPPC(10%): DSPE-PEG(2000) (4%) and POPC:MPPC(10%):DSPE-PEG(2000) (4%) membranes as a function of temperature.

to the presence of lysolipid in the liquid state membranes (i.e. free volume), the permeability rates should coincide in this region. That the permeabilities of the two different compositions do not match add support to the conclusion that the enhancement is due to the presence of residual interfacial areas with lysolipid-stabilized pores in the DPPC-Lysolipid containing systems. The transition temperature of POPC vesicles is − 2 °C, so they do not have any interfacial regions at, what is then, over 40 °C above this temperature for the stabilized pores to form.

One last supporting piece of evidence for the proposed presence of interfacial areas (and lysolipid pores) extending into the liquid phase region of the LTSLs comes from mechanical measurements of lysolipid containing EggPC vesicles. Zhelev has measured the area expansion modulus of monooleoylphosphatidylcholine (MOPC):EggPC (10–30% lysoPC) bilayers and determined that the intrinsic area expansion modulus of MOPC is ~150 mN/m, almost identical to the modulus for pure EggPC (~170 mN/m) [64]. Therefore, a linear combination of the two lipids, and moduli, e.g., K_aMixture=K_aMOPC(10%)+K_aEggPC(90%) would also produce a modulus of ~150–170 mN/m. As noted above, a decrease in modulus (increased compressibility) relates directly to an increase in permeability. If the presence of 10% MOPC does not significantly lower the modulus of a liquid state bilayer, it should not significantly increase the permeability (i.e., the only small enhancement noted with MPPC in POPC), as observed, but it does play a role at the remaining solid–liquid boundaries in the obstensibly liquid state membrane.

From TLC and NMR analysis, very little, if any, lysolipid appears to desorb from liquid phase membranes even when held in dialysis at a temperature of ~45–48 °C for 48 h (although a truly quantitative measurement is still lacking, and it is possible that dialysis may not remove the very small amounts of desorbed lysolipid from the vesicle suspension). At first glance, this finding conflicts with the lysolipid absorption/desorption data of Zhelev and Needham [21,35] where they showed uptake and then washout of lysolipid from liquid phase vesicles using the flow micropipette technique. In the case of the flow pipette experiments though, lysolipid was introduced into large (~20 μm), unilamellar vesicles in situ. From area change measurements observed on these giant vesicles, initial uptake is into the outer monolayer occurred at a rate of ~0.2/s. Both sides of the membranes expanded, and eventually lysolipid flipped at a slower rate (0.002/s) to the inner monolayer. Desorption, though (~0.2/s), was only observed from the outer monolayer at short times before significant lipid was able to flip and populate the inner monolayer [21,35].

In contrast, the vesicles used in the present experiments were 100 nm in diameter and prepared with lysolipid already in the membrane at 10 mol% (i.e. ~10% in each monolayer). For lysolipid to desorb, it first must leave from the outer monolayer at a rate 100 times faster than the transfer across the bilayer. For this to occur, the outer monolayer must compress compared to the inner monolayer and this would be expected to make the membrane bend inwards to accommodate the loss of material (area and volume) from the outer monolayer. Presumably, the energy required for this "buckling" to take place is so high relative to the chemical potential of lysolipid in solution that it does not occur, so lysolipid remains in both sides of the membrane and does not desorb.

It is important to note that the conical geometry of the lysoPCs is crucial, as it allows them to form the required, highly curved, hemispherical shape of the pore. We have also measured dithionite permeability through DPPC membranes that contained 10 mol% of monopalmitoyl-glycerol (GMP). This molecule is identical to MPPC (single C16 chain, glycerol backbone), except that it does not have the relatively bulky PC head group. Permeability results (data not shown) indicated no enhancement of dithionite permeability compared to pure DPPC, indicating that presumably, GMP was not able to stabilize porous defect structure, as MPPC was. The geometry of the GMP molecule is more "cylindrical" or even inverse-conical without the large PC headgroup, and as such, it would not be expected to form and stabilize the highly curved sides of the membrane pore having intrinsically the opposite curvature. In addition, the molecule is highly hydrophobic, so it is unlikely that it would form a water lined structure through the membrane and certainly should not desorb. A recent paper from Langer and Hui has measured the dithionite ion permeability through DimyristoylPC (DMPC-diC14) vesicles at their transition temperature (~24 °C) with and without free fatty acids [33]. For pure DMPC vesicles, the ions cross the membrane rapidly, quenching all of the NBD-fluorescent molecules within ~2–3 min. The addition of 10 mol% stearic acid to the membrane reduces the permeability rate by a factor of ~2 while the addition of the unsaturated oleic fatty acid reduced the rate almost 10-fold. Not only does the addition of a single fatty acid chain not enhance the permeability, but its presence in the membrane interfacial region actually retards ion permeability. This data again support the proposal that the favorably conical shaped lysolipid and its ability to form head group lined membrane pores are essential for the enhanced permeability.

5. Conclusion

The results from this work provide some support to the hypothesis that the rapid release of contents from LTSL membranes occurs through lysolipid-stabilized pores at grain boundary regions in otherwise intact membranes at their main acyl melting transition region. It should be noted though that the presence of pores has not been absolutely proven by this data. Measurements of dithionite permeability and Doxorubicin release indicate permeability rate enhancement begins several degrees below the peak of the thermal transition, and extends several degrees past it. These results are in line with, and support, the interfacial permeability models of Mouritsen that predict the presence of interfacial solid–liquid boundary regions both before and after the main calorimetric peak. Although some lysolipid desorption from liquid state membranes cannot be ruled out, it appears that lysolipid must remain in the membrane for the permeability enhancement. It should be noted that lysolipid desorption has not been completely ruled out as a mechanism for enhanced permeability at the phase transition. The results from both the particle size analysis and the temperature cycling study with the micropipette indicate that LTSLs remain as intact bilayers during the phase transition, as well as after several cycles through T_m. It appears the permeability enhancement mechanism is lysolipid pore stabilization, and not a result of complete destruction or micellization of the vesicles.

Acknowledgements

We would like to thank Dr. Anthony Ribeiro of the Duke University Shared Magnetic Resonance Facility for his assistance with the NMR analysis, as well as Dr. Mark Grinstaff and his laboratory for their help with the TLC analysis. We would also like to thank Dr. Patrick Kiser and Dr. Doncho Zhelev for many helpful suggestions and discussions. We would like to acknowledge support for this project from NIH grants GM40162 and CA87630, and NSF grant CDR-8622201.

References

[1] D. Paphadjopoulos, K. Jacobsen, S. Nir, T. Isac, Phase transitions in phospholipid vesicles. Fluorescence polarization and permeability measurements concerning the effects of temperature and cholesterol, Biochim. Biophys. Acta 311 (1973) 330–348.
[2] O.G. Mouritsen, K. Jorgensen, T. Honger, Permeability of lipid bilayers near the phase transition, in: E.A. Disalvo, S.A. Simon (Eds.), Permeability and Stability of Lipid Bilayers, CRC Press, Boca Raton, 1995, pp. 137–160.
[3] J.F. Nagle, H.L. Scott, Lateral compressibility of lipid mono- and bilayers theory of membrane permeability, Biochim. Biophys. Acta 513 (1978) 236–243.
[4] S. Doniach, Thermodynamic fluctuations in phospholipid bilayers, J. Chem. Phys. 68 (1978) 4912–4916.
[5] E. Evans, R. Kwok, Mechanical calorimetry of large dimyristoylphosphatidylcholine vesicles in the phase transition region, Biochemistry 21 (1982) 4874–4879.
[6] D. Marsh, A. Watts, P.F. Knowles, Evidence for phase boundary lipid. Permeability of temp-choline into dimyristoylphosphatidylcholine vesicles at the phase transition, Biochemistry 15 (1976) 3570–3578.
[7] E. Corvera, O.G. Mouritsen, M.A. Singer, M.J. Zuckerman, The permeability and the effect of acyl-chain length for phospholipid bilayers containing cholesterol: theory and experiment, Biochim. Biophys. Acta 1107 (1991) 261–270.
[8] O.G. Mouritsen, M.J. Zuckermann, Model of interfacial melting, Phys. Rev. Lett. 58 (1987) 389–392.
[9] J.F. Shackelford, Introduction to Materials Science for Engineers, Macmillan Publishing Company, New York, 1988.
[10] D.H. Kim, M.J. Costello, B. Duncan, D. Needham, Mechanical properties and microstructure of polycrystalline phospholipid monolayer shells: novel solid microparticles, Langmuir 19 (2003) 8455–8466.
[11] D. Needham, M. Dewhirst, Review: the development and testing of a new temperature-sensitive drug delivery system for the treatment of solid tumors, Adv. Drug Delivery Rev. 53 (2001) 285–305.
[12] L.M. Ickenstein, M.C. Arfvidsson, D. Needham, L.D. Mayer, K. Edwards, Disc formation in cholesterol-free liposomes during phase transition, Biochim. Biophys. Acta 1614 (2003) 135–138.
[13] L. Cruzeiro-Hansson, O.G. Mouritsen, Passive ion permeability of lipid membranes modelled via lipid-domain interfacial area, Biochim. Biophys. Acta 944 (1988) 63–72.
[14] J.A. Reynolds, C. Tanford, W.L. Stone, Interaction of L-alpha-didecanoyl phosphatidylcholine with the AI polypeptide of high density lipoprotein, Proc. Natl. Acad. Sci. U. S. A. 74 (1977) 3796–3799.
[15] J. Risbo, K. Jorgensen, M.M. Sperotto, O.G. Mouritsen, Phase behavior and permeability properties of phospholipid bilayers containing a short-chain phospholipid permeability enhancer, Biochim. Biophys. Acta 1329 (1997) 85–96.
[16] D. Needham, G. Anyarambhatla, G. Kong, M.W. Dewhirst, A new temperature-sensitive liposome for use with mild myperthermia: characterization and testing in a human tumor xenograft model, Cancer Res. 60 (2000) 1197–1201.
[17] G.R. Anyarambhatla, D. Needham, Enhancement of the phase transition permeability of DPPC liposomes by incorporation of MPPC: a new temperature-sensitive liposome for use with mild hyperthermia, J. Liposome Res. 19 (1999) 491–506.
[18] C.J.A. Van Echteld, B. De Kruijff, J.G. Mandersloot, J. De Gier, Effects of lysophosphatidylcholines on phosphatidylcholine and phosphatidylcholine/cholesterol liposome systems as revealed by ^{31}P-NMR, electron microscopy and permeability studies, Biochim. Biophys. Acta 649 (1981) 211–220.
[19] W. Kramp, G. Pieron, R.N. Pincard, D.J. Hanahan, Observations on the critical micellar concentrations of 1-0-Alkyl-2-Acetyl-sn-Glycero-3-phosphocholine and a series of its homologs and analogs, Chem. Phys. Lipids 35 (1984) 49–62.
[20] M.E. Haberland, J.A. Reynolds, Interaction of L-alpha-palmitoyl lysophosphatidylcholine with the AI polypeptide of high density lipoprotein, J. Biol. Chem. 250 (1975) 6636–6639.
[21] D. Needham, D.V. Zhelev, Lysolipid exchange with lipid vesicle membranes, Ann. Biomed. Eng. 23 (1995) 287–298.
[22] D. Needham, N. Stoicheva, D.V. Zhelev, Exchange of monooleoylphosphatidycholine as monomer and micelle with membranes containing grafted poly(ethyleneglycol)-lipid, Biophys. J. 73 (1997) 2615–2629.
[23] D. Marsh, CRC Handbook of Lipid Bilayers, CRC Press, Boca Raton, 1990.
[24] R.T. Hamilton, E.W. Kaler, Alkali metal ion transport through thin bilayers, J. Phys. Chem. 94 (1990) 2560–2566.
[25] D. Papahadjopoulos, A. Bangham, Biophysical properties of phospholipids: II. Permeability of phosphatidylserine liquid crystals to univalent ions, Biochim. Biophys. Acta 126 (1966) 185–188.
[26] D.D. Perrin, Ionisation Constants of Inorganic Acids and Bases in Aqueous Solution, Pergamon Press, Oxford, 1982.
[27] C.R. Wasmuth, C. Edwards, R. Hutcherson, Participation of the SO_2^- radical ion in the reduction of p-nitrophenol by sodium dithionite, J. Phys. Chem. 68 (1964) 423–425.
[28] J.C. McIntyre, R.G. Sleight, Fluorescence assay for phospholipid membrane asymmetry, Biochemistry 30 (1991) 11819–11827.
[29] C. Angeletti, J.W. Nichols, Dithionite quenching rate measurements of the

inside–outside membrane bilayer distribution of 7-nitrobenz-2-oxa-1,3-diazol-4-yl-labeled phospholipids, Biochemistry 37 (1998) 15114–15119.
[30] C. Balch, R. Morris, E. Brooks, R.G. Sleight, The use of N-(7-nitrobenz-2-oxa-1,3-diasole-4-yl)-labeled lipids in determining transmembrane lipid distribution, Chem. Phys. Lipids 70 (1994) 205–212.
[31] R.E. Pagano, O.C. Martin, A.J. Schroit, D.K. Struck, Formation of asymmetric phospholipid membranes via spontaneous transfer of fluorescent lipid analogues between vesicle populations, Biochemistry 20 (1981) 4920–4927.
[32] M. Langner, S.W. Hui, Dithionite penetration through phospholipid bilayers as a measure of defects in lipid molecular packing, Chem. Phys. Lipids 65 (1993) 23–30.
[33] M. Langner, S.W. Hui, Effect of free fatty acids on the permeability of 1,2-dimyrisoyl-*sn*-glycero-3-phosphocholine bilayer at the main phase transition, Biochim. Biophys. Acta 1463 (2000) 439–447.
[34] D. Needham, E. Evans, Structure and mechanical properties of giant lipid (DMPC) vesicle bilayers from 20 °C below to 10 °C above the liquid-crystalline phase transition at 24 °C, Biochemistry 27 (1988) 8261–8269.
[35] D. Zhelev, Exchange of monooleoylphosphatidylcholine with single egg phosphatidylcholine vesicle membranes, Biophys. J. 71 (1996) 257–273.
[36] E. Evans, D. Needham, Physical properties of surfactant bilayer membranes: thermal transitions, elasticity, rigidity, cohesion, and colloidal interactions, J. Phys. Chem. 91 (1987) 4219–4228.
[37] D. Needham, T.J. McIntosh, E.A. Evans, Thermomechanical and transition properties of dimyristoylphosphatidylcholine/cholesterol bilayers, Biochemistry 27 (1988) 4668–4673.
[38] K. Olbrich, W. Rawicz, D. Needham, E. Evans, Water permeability and mechanical strength of polyunsaturated lipid bilayers, Biophys. J. 79 (2000) 321–327.
[39] W. Rawicz, K.C. Olbrich, T. McIntosh, D. Needham, E. Evans, Effect of chain length and unsaturation on elasticity of lipid bilayers, Biophys. J. 79 (2000) 328–339.
[40] R. Kwok, E. Evans, Thermoelasticity of large lecithin bilayer vesicles, Biophys. J. 35 (1981) 637–652.
[41] L.D. Mayer, M.B. Bally, P.R. Cullis, Uptake of adriamycin into large unilamellar vesicles in response to a pH gradient, Biochim. Biophys. Acta 857 (1986) 123–126.
[42] T.D. Madden, P.R. Harrigan, L.C.L. Tai, M.B. Bally, L.D. Mayer, T.E. Redelmeier, H.C. Loughrey, C.P.S. Tilcock, L.W. Reinish, P.R. Cullis, The accumulation of drugs within large unilamellar vesicles exhibiting a proton gradient: a survey, Chem. Phys. Lipids 53 (1990) 37–46.
[43] L.D. Mayer, L.C.L. Tai, M.B. Bally, G.N. Mitilenes, R.S. Ginsberg, P.R. Cullis, Characterization of liposomal systems containing doxorubicin entrapped in response to pH gradients, Biochim. Biophys. Acta 1025 (1990) 143–151.
[44] M.H. Gaber, K. Hong, S.K. Huang, D. Papahadjopoulos, Thermosensitive sterically stabilized liposomes: formulation and in vitro studies on mechanism of doxorubicin release by bovine serum and human plasma, Pharm. Res. 12 (1995) 1407–1416.
[45] X. Li, D.J. Hirsh, D. Cabral-Lilly, A. Zirkel, S.M. Gruner, A.S. Janoff, W.R. Perkins, Doxorubicin physical state in solution and inside liposomes loaded via a pH gradient, Biochem. Biophys. Acta 14 (1998) 23–40.
[46] B. Fried, J. Sherma, Thin-Layer Chromatography: Techniques and Applications, Marcel Dekker, Inc., New York, 1994.
[47] A. Ault, NMR An Introduction to Proton Nuclear Magnetic Resonance Spectroscopy, Holden-Day, Inc, San Francisco, 1976.
[48] M. Bloom, E. Evans, O.G. Mouritsen, Physical properties of the fluid lipid-bilayer component of cell membranes: a perspective, Q. Rev. Biophys. 24 (1991) 293–397.
[49] A. Finkelstein, Water Movement Through Lipid BIlayers, Pores and Plasma Membranes: Theory and Reality, Wiley Interscience, New York, 1987.
[50] I.W.M. Smith, Kinetics and Dynamics of Elementary Gas Reactions, Butterworths, London, 1980.
[51] W. Stiller, Arrhenius Equation and Non-Equilibrium Kinetics, Teubner-Texte zur Physik, Berlin, 1989.
[52] K. Olbrich, Water Permeability and Mechanical Properties of Unsaturated Lipid Membranes and Sarcolemmal Vesicles, Doctoral Dissertation in Mechanical Engineering and Materials Science, Duke University: Durham, NC, 1997.
[53] G. Cevc, D. Marsh, Phospholipid Bilayers. Physical Principles and Models, John Wiley and Sons, New York, 1987.
[54] R.A. GusKova, I.A. Ivanov, V.K. KolTover, V.V. Akhobadze, A.B. Rubin, Permeability of bilayer lipid membranes for superoxide (O_2^-) radicals, Biochim. Biophys. Acta 778 (1984) 579–585.
[55] B.E. Cohen, The permeability of liposomes to nonelectrolytes, J. Membr. Biol. 20 (1975) 205–234.
[56] R.A. Moss, S. Bhattacharya, Transverse membrane asymmetry in model phospholipid bilayers: NBD-phosphatidylethanolamine and the separation of flip from flop, J. Am. Chem. Soc. 117 (1995) 8688–8689.
[57] A.J. Bangham, J.E. Lea, The interaction of detergents with bilayer lipid membranes, Biochim. Biophys. Acta 511 (1978) 388–396.
[58] L.M. Hays, J.H. Crowe, W. Wolkers, S. Rudenko, Factors affecting leakage of trapped solutes from phospholipid vesicles during thermotropic phase transitions, Cryobiology 42 (2001) 88–102.
[59] S. Paula, A.G. Volkov, D.W. Deamer, Permeation of halide anions through phospholipid bilayers occurs by the solubility-diffusion mechanism, Biophys. J. 74 (1998) 319–327.
[60] M. Jansen, A. Blume, A comparative study of diffusive and osmotic water permeation across bilayers composed of phospholipids with different head groups and fatty acyl chains, Biophys. J. 68 (1995) 997–1008.
[61] T.J. McIntosh, S. Advani, R.E. Burton, D.V. Zhelev, D. Needham, Experimental tests for protrusion and undulation pressures in phospholipid bilayers, Biochemistry 34 (1995) 8520–8532.
[62] A. Jutila, P.K.J. Kinnunen, Novel features of the main transition of dimyristoylphosphocholine bilayers revealed by fluorescence spectroscopy, J. Phys. Chem. 101 (1997) 7635–7640.
[63] J. Israelachvili, Intermolecular and Surface Forces, vol. 2, Academic Press, San Diego, 1992.
[64] D. Zhelev, Material property characteristics for lipid bilayers containing lysolipid, Biophys. J. 75 (1998) 321–330.
[65] A.C. Chakrabarti, D.W. Deamer, Permeability of lipid bilayers to amino acids and phosphate, Biochim. Biophys. Acta 1111 (1992) 171–177.
[66] Q. Chen, S. Tong, M. Dewhirst, F. Yuan, Targeting tumor microvessels using doxorubicin encapsulated in a novel thermosensitive liposome, Mol. Cancer Ther. 3 (2004) 1311–1317.